ChemPubSoc Europe

DOI: 10.1002/ejic.201600441

EurJIC European Journal of Inorganic Chemistry

Full Paper

Ring-Opening Polymerization

Magnesium and Zinc Complexes Supported by N,N,O Tridentate Ligands: Synthesis and Catalysis in the Ring-Opening Polymerization of *rac*-Lactide and α-Methyltrimethylene Carbonate

Miao Huang[a] and Haiyan Ma*[a]

Abstract: A series of racemic biphenyl- or binaphthyl-based aminophenols were treated with 1 equiv. of $Mg[N(SiMe_3)_2]_2$ or $Zn[N(SiMe_3)_2]_2$ to provide eight heteroleptic magnesium and zinc silylamido complexes (Mg, **1a**–**5a**; Zn, **1b**, **3b**, **5b**). Single-crystal X-ray diffraction studies on typical magnesium complex **5a** and zinc complexes **1b**, **3b**, and **5b** showed a tridentate chelating mode of the ligand and a distorted tetrahedral geometry around the metal center. All of these complexes proved to be efficient initiators for the ring-opening polymerization of *rac*-lactide in toluene and THF. Microstructure analysis of the resultant poly(*rac*-lactide) samples by homonuclear-decoupled ^1H NMR spectroscopy revealed heterotacticities ranging from 0.45 to 0.69. These complexes were also applied as initiators in the polymerization of racemic α-methyltrimethylene carbonate in toluene and exhibited moderate to high regioselectivities; the most regioregular polymer was obtained with magnesium complex **4a** (X_{reg} = 0.93).

Introduction

Polylactides (PLAs) and poly(α-methyltrimethylene carbonate)s [P(α-MeTMC)s], as important biodegradable and biocompatible polymers, are considered to be ideal alternatives to petroleum-based plastics.[1,2] The applications of these polymers are intimately related to their microstructures, and the ring-opening polymerization (ROP) of the corresponding cyclic monomers in racemic form catalyzed by metal-based initiators is the most efficient route to obtain PLAs and P(α-MeTMC)s with predictable molecular weights, narrow molecular weight distributions, and stereo-/regiotacticities.[3,4] Hence, designing well-defined metal catalysts to prepare PLAs or P(α-MeTMC)s with specific architectures has become a major focus of attention in recent years.

A large number of metal complexes based predominantly (but not exclusively) on alkali metals,[5–7] aluminum,[8–15] iron,[16,17] titanium,[18–20] zirconium,[21,22] magnesium,[23–35] zinc,[30–42] calcium,[43–46] and trivalent lanthanides[47–50] have been reported to be effective catalysts/initiators for the ROP of lactides. Among them, aluminum complexes, especially those supported by salen-type ligands and their derivatives, exhibit satisfactory isoselectivities toward *rac*-lactide (*rac*-LA) polymerization, which is highly desired for obtaining PLAs with enhanced thermal properties.[8–10] Nevertheless, the generally low activity of aluminum initiators restricts their practical applications to some extent. Under these circumstances, the high activity of magnesium and zinc species, coupled with the nontoxicity and low cost of these elements, attracted our attention. Although the stereoselectivity control in the ROP of *rac*-LA initiated by magnesium and zinc initiators is still not well established, it is expected that these elements will provide good potential to afford highly isoselective and active initiators, since a few magnesium complexes with high heteroselectivity and zinc complexes with high hetero-/isoselectivity towards the ROP of *rac*-LA have been reported. For instance, magnesium complexes bearing phosphinimino amine ligands showed high heteroselectivity (P_r = 0.98).[51] Zinc β-diketiminate complexes exhibited high heteroselectivity (P_r = 0.87),[52] and amido-oxazolinate zinc silylamido complexes showed high isoselectivity (P_m = 0.91).[53] Currently, more and more efforts are being devoted to the development of new stereoselective zinc and magnesium initiators, particularly those that can produce isotactic PLAs from *rac*-LA.

Polycarbonates are another type of biobased aliphatic polyesters. Various discrete metal complexes have been employed in the ROP of trimethylene carbonate (TMC),[54–57] but the polymerization of similar chiral cyclic carbonates, such as α-MeTMC, has seldom been explored. Yasuda and co-workers reported the ROP of (*R*)-α-MeTMC catalyzed by various types of initiators, such as $AlEt_3$–H_2O, $Sn(Oct)_2$, $[(C_5Me_5)_2Sm(thf)_2]$, and $[(C_5Me_5)_2SmMe(thf)]$, in toluene.[58] Rare earth metal alkoxides or aryloxides ["$Ln(OiPr)_3$"; $Ln(OAr)_3$, Ar = 2,6-di-*tert*-butyl-4-methylphenolate; Ln = La, Dy, Y] were also reported for the polymerization of this monomer, which afforded polycarbon-

[a] *Shanghai Key Laboratory of Functional Materials Chemistry and Laboratory of Organometallic Chemistry, East China University of Science and Technology,*
130 Meilong Road, Shanghai 200237, P. R. China
E-mail: haiyanma@ecust.edu.cn
http://webmanage.ecust.edu.cn/s/230/t/262/a/57290/info.jspy

Supporting information for this article is available on the WWW under http://dx.doi.org/10.1002/ejic.201600441.

ates with high molecular weights and moderate polydispersities.[59] [(BDI*i*Pr)ZnN(SiMe$_3$)$_2$] can also effectively initiate the ROP of α-MeTMC and shows high regioselectivity (X_{reg} > 0.98).[60] We reported a series of magnesium silylamido complexes bearing biphenyl-based iminophenolate ligands, which showed moderate activities for the ROP of α-MeTMC, affording regioregular polymers (X_{reg} = 0.65–0.86).[61] Nevertheless, in comparison with catalyst systems for *rac*-LA polymerization, those involved in α-MeTMC polymerization are still rather limited.

Previously, we synthesized a series of magnesium and zinc silylamido complexes supported by racemic binaphthyl-based iminophenolate ligands, which showed moderate heteroselectivities toward the polymerization of *rac*-LA (P_r = 0.72–0.84) and moderate to high regioselectivities toward the polymerization of racemic α-MeTMC (X_{reg} = 0.78–0.98).[62] The NMe$_2$ group on the binaphthyl ring of these complexes is dissociated from the metal center in solution, and this is considered to weaken the chiral induction effect of the binaphthyl moiety during the polymerization. Therefore, in this work we synthesized an array of magnesium and zinc complexes derived from relatively flexible aminophenolate ligands based on two types of chiral backbones (racemic dimethylaminobiphenyl and dimethylaminobinaphthyl backbones), which proved to wrap around the metal center in a more efficient manner. Detailed data concerning their catalytic behavior toward the polymerization of *rac*-LA and racemic α-MeTMC are presented.

Results and Discussion

The synthetic strategies for the biphenyl-based aminophenol proligands **L$^{1-4}$H** are summarized in Scheme 1. The synthesis of *N*′,*N*′-dimethyl-1,1′-biphenyl-2,2′-diamine was based on a modified procedure.[61] Then acetylation of this diamine followed by reduction with LiAlH$_4$ afforded the corresponding *N*-ethyl-*N*′,*N*′-dimethyl-1,1′-biphenyl-2,2′-diamine (see Supporting Information). *N*-Ethyl-*N*′,*N*′,6,6′-tetramethyl-1,1′-biphenyl-2,2′-diamine was synthesized similarly (see Supporting Information). Coupling reactions of these two *N*-ethyl-substituted amines with different benzyl bromide derivatives yielded the target dimethylaminobiphenyl-based aminophenol proligands **L$^{1-4}$H**. Similar synthetic strategies were adopted to obtain the binaphthyl-based aminophenol proligand **L^{5}H** (Scheme 2). All the obtained biphenyl- and binaphthyl-based aminophenols are colorless crystalline solids, which were characterized via ^{1}H and ^{13}C NMR spectroscopy and elemental analysis.[63]

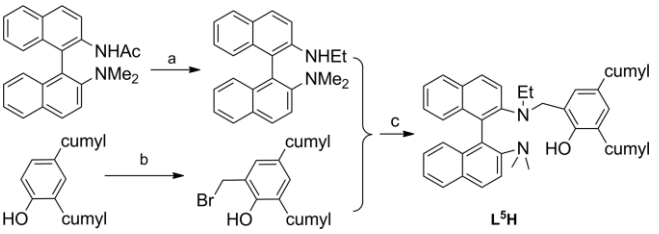

Scheme 2. Synthesis of proligand **L^{5}H**. (a) LiAlH$_4$, THF, reflux. (b) (HCHO)$_n$, HBr, HOAc, 70 °C. (c) Et$_3$N, THF, room temp.

The heteroleptic magnesium silylamido complexes **1a**–**5a** were prepared by reaction of Mg[N(SiMe$_3$)$_2$]$_2$ with 1 equiv.of the corresponding aminophenol proligands **L$^{1-5}$H** in toluene at ambient temperature via an amine-elimination route (Scheme 3).[64] Colorless crystalline solids were obtained after recrystallization from toluene/*n*-hexane at room temp. Although these magnesium complexes have two stereogenic centers (the skeleton N atom and the metal center) in addition to the chiral biphenyl or binaphthyl moiety, only a pair of enantiomers was formed, as evidenced by the appearance of a single set of resonances corresponding to the stoichiometric structures of these complexes.

Similar reactions of proligands **L$^{1-5}$H** with Zn[N(SiMe$_3$)$_2$]$_2$ were carried out to synthesize the corresponding zinc complexes (Scheme 3).[64] Zinc silylamido complexes **1b**, **3b**, and **5b** could be isolated as colorless solids in moderate yields. Unexpectedly, the reactions of equimolar amounts of **L^{2,4}H** and Zn[N(SiMe$_3$)$_2$]$_2$ gave a mixture of mono- and bis-ligated complexes. Exhaustive fractional crystallization failed to afford the target heteroleptic zinc silylamido complexes in pure form. Similar to the magnesium complexes, no diastereomers could be observed in the ^{1}H NMR spectra of these zinc complexes.

The ^{1}H NMR spectra of magnesium complexes **1a**–**5a** and zinc complexes **1b**, **3b**, **5b** in C$_6$D$_6$ at room temperature demonstrate that the N(CH$_3$)$_2$ group in the ligand framework is well coordinated to the metal center in these complexes. For instance, in the ^{1}H NMR spectra, the sharp signal of the N(CH$_3$)$_2$ protons of the free ligand **L^{1}H** appears at δ = 2.09 ppm, while

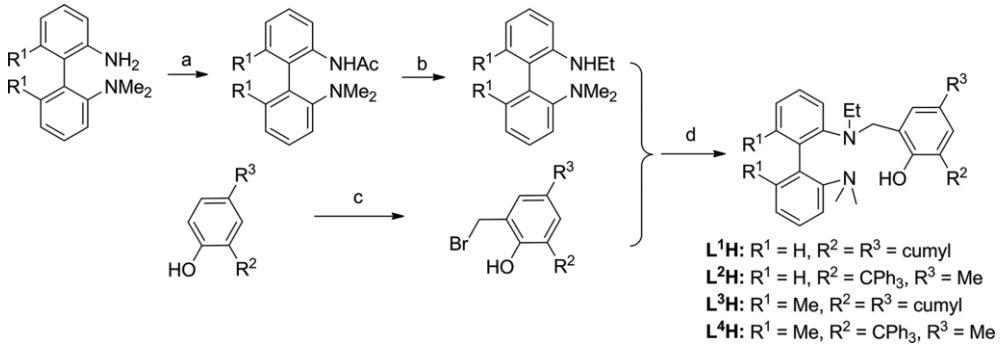

Scheme 1. Synthesis of proligands **L^{1}H**–**L^{4}H**. (a) Ac$_2$O, HOAc, CH$_2$Cl$_2$, room temp. (b) LiAlH$_4$, THF, reflux. (c) (HCHO)$_n$, HBr, HOAc, 70 °C. (d) Et$_3$N, THF, room temp.

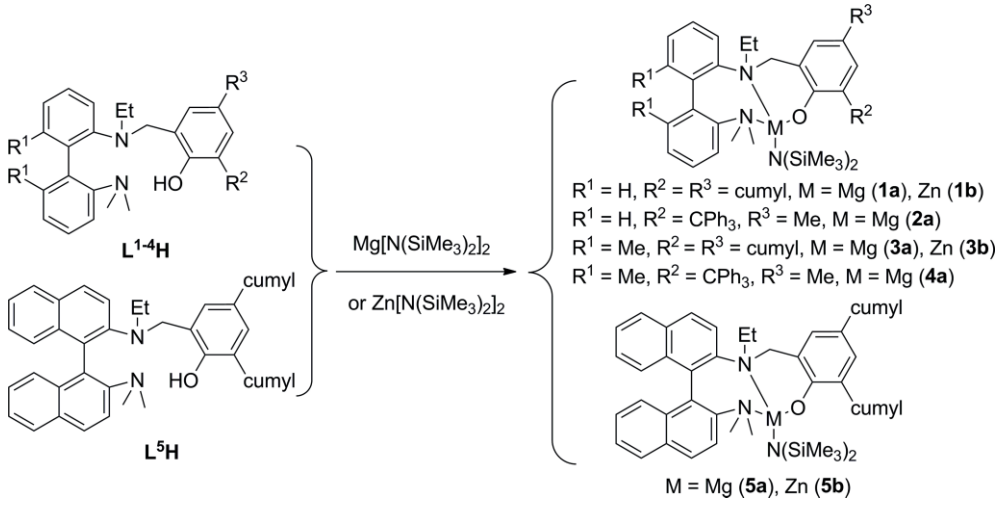

Scheme 3. Synthesis of magnesium and zinc silylamido complexes.

two signals of $N(CH_3)_2$ protons of complex **1a** are observed at δ = 2.46 ppm and 1.60 ppm, with one resonance shifted significantly to the high-field region. Similar phenomena are also observed in the ^{1}H NMR spectra of **2a**–**5a** and **1b**, **3b**, **5b** in C_6D_6. Therefore, it is conceivable that these magnesium and zinc complexes have the same configuration in solution as in the solid state (see below). This is in contrast to our previously reported binaphthyl-based iminophenolate magnesium complexes, for which dissociation of the amino group was witnessed in solution,[62] and implies the formation of a less flexible complex geometry in this work.

Crystallographic Studies

Single crystals of magnesium complex **5a** and zinc complexes **1b**, **3b**, and **5b** suitable for X-ray structure determination were obtained from saturated solutions in *n*-hexane/toluene at room temperature. The crystallographic data and refinement of these complexes are listed in Table 1, and the ORTEPs of the molecular structures of these complexes are shown in Figures 1, 2, 3, and 4.

As shown in Figure 1, complex **5a** has a monomeric structure in the solid state in which the magnesium center is fourfold

Table 1. Crystallographic data and refinement for **5a**, **1b**, **3b** and **5b**.

	5a	**1b**	**3b**	**5b**
Empirical formula	$C_{55}H_{67}MgN_3OSi_2$	$C_{47}H_{63}N_3OSi_2Zn$	$C_{55}H_{81}N_3OSi_2Zn$	$C_{55}H_{67}N_3OSi_2Zn$
Formula weight	866.60	807.55	921.78	907.66
T [K]	293(2)	140(2)	140(2)	293(2)
Crystal size [mm]	0.26 × 0.21 × 0.13	0.20 × 0.12 × 0.10	0.24 × 0.13 × 0.08	0.243 × 0.211 × 0.134
Crystal system	triclinic	triclinic	triclinic	triclinic
Space group	$P\bar{1}$	$P\bar{1}$	$P\bar{1}$	$P\bar{1}$
a [Å]	12.278(2)	13.2300(18)	13.0326(16)	12.252(8)
b [Å]	15.122(3)	13.3702(18)	14.5796(18)	15.016(10)
c [Å]	17.749(3)	15.751(2)	16.981(2)	17.599(12)
α [°]	97.615(4)	80.986(3)	104.916(2)	98.158(13)
β [°]	100.073(4)	82.522(3)	103.356(2)	99.532(14)
γ [°]	111.948(3)	66.010(2)	104.166(2)	112.005(11)
V [Å^3]	2937.9(9)	2507.2(6)	2870.4(6)	2886(3)
Z	2	2	2	2
$\varrho_{calcd.}$ [Mg/m^3]	0.980	1.070	1.067	1.045
Absorption coeff. [mm^{-1}]	0.106	0.570	0.505	0.502
F (000)	932	864	996	968
θ range [°]	1.69 to 26.00	1.31 to 30.78	1.53 to 27.00	1.70 to 25.05
Data collection (*hkl*)	–10 to 15, ±18, ±21	–18 to 19, ±19, –22 to 17	±16, ±18, –21 to 15	–12 to 14, –17 to 16, –20 to 15
Reflections collected/unique	17405/11500	25780/15378	22000/12411	15325/10136
R (int)	0.0352	0.0790	0.0366	0.0814
Max. / min. transmission	1.0000 / 0.0962	0.9452 / 0.8945	0.9607 / 0.8883	1.00000 / 0.2654
Data/restrains/parameters	11500/14/572	15378/0/500	12411/31/576	10136/24/572
Goodness of fit on F^2	1.036	0.906	1.073	0.965
Final R_1,wR_2 [$I > 2\sigma(I)$]	0.0582, 0.1472	0.0672, 0.1247	0.0561, 0.1683	0.0814, 0.1926
R_1, wR_2 (all data)	0.1081, 0.1687	0.1633, 0.1423	0.0787, 0.1963	0.1454, 0.2202
$\Delta\varrho_{max./min.}$ [e Å^{-3}]	0.333/–0.266	0.447/–0.385	0.661/–0.609	1.104/–1.029

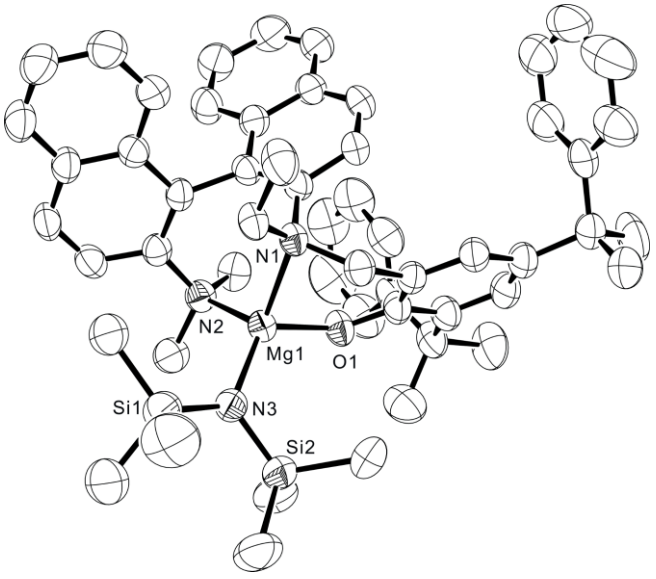

Figure 1. ORTEP of the molecular structure of [(L^5)MgN(SiMe$_3$)$_2$] (**5a**). Thermal ellipsoids are drawn at 50 % probability. Selected bond lengths [Å] and angles [°]: Mg1–O1 1.9245(16), Mg1–N1 2.228(2), Mg1–N2 2.202(2), Mg1–N3 2.036(2); O1–Mg1–N3 120.87(9), O1–Mg1–N2 98.94(8), N3–Mg1–N2 115.37(8), O1–Mg1–N1 92.19(7), N3–Mg1–N1 116.62(8), N2–Mg1–N1 109.51(8).

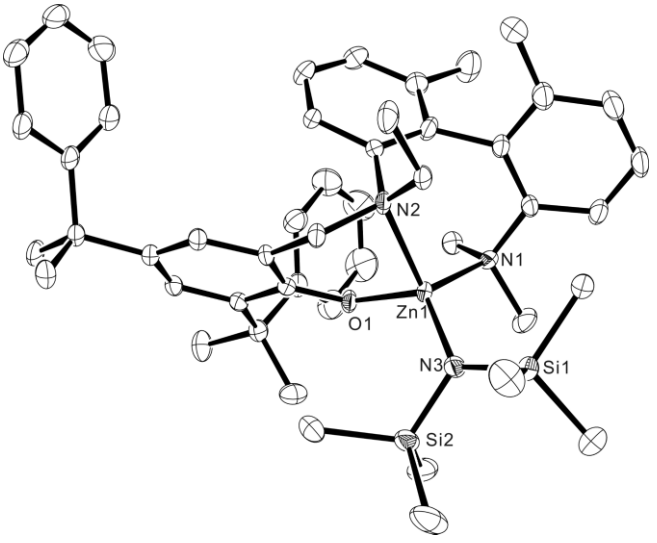

Figure 3. ORTEP of the molecular structure of [(L^3)ZnN(SiMe$_3$)$_2$] (**3b**). Thermal ellipsoids are drawn at 50 % probability. Selected bond lengths [Å] and angles [°]: Zn1–O1 1.917(2), Zn1–N1 2.153(3), Zn1–N2 2.146(3), Zn1–N3 1.940(2); O1–Zn1–N3 121.18(10), O1–Zn1–N2 93.13(9), N3–Zn1–N2 116.06(11), O1–Zn1–N1 95.11(9), N3–Zn1–N1 118.64(10), N2–Zn1–N1 108.35(10).

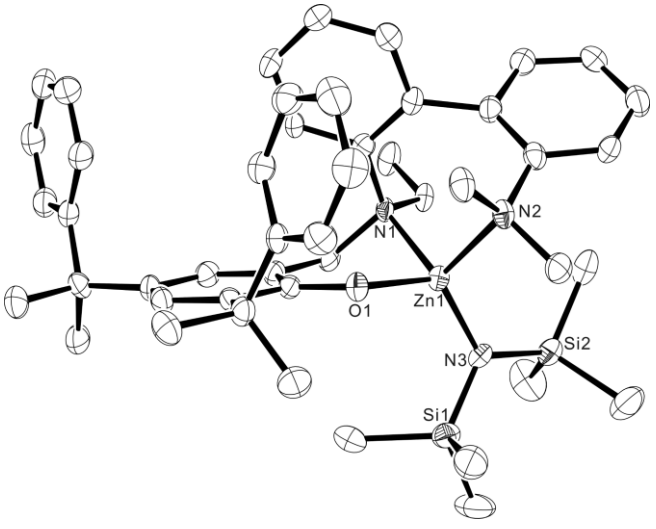

Figure 2. ORTEP of the molecular structure of [(L^1)ZnN(SiMe$_3$)$_2$] (**1b**). Thermal ellipsoids are drawn at 50 % probability. Selected bond lengths [Å] and angles [°]: Zn1–O1 1.918(2), Zn1–N1 2.152(3), Zn1–N2 2.132(3), Zn1–N3 1.933(3); O1–Zn1–N3 123.31(11), O1–Zn1–N2 95.97(10), N3–Zn1–N2 118.92(12), O1–Zn1–N1 92.26(10), N3–Zn1–N1 114.53(11), N2–Zn1–N1 107.52(11).

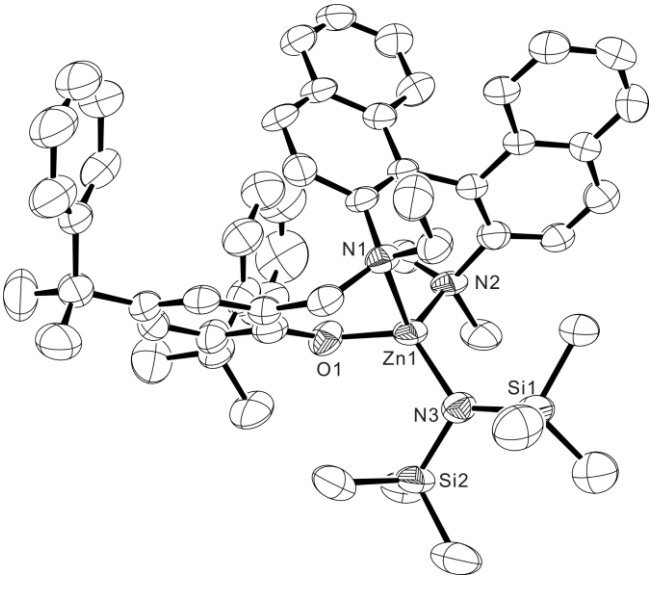

Figure 4. ORTEP of the molecular structure of [(L^5)ZnN(SiMe$_3$)$_2$] (**5b**). Thermal ellipsoids are drawn at 50 % probability. Selected bond lengths [Å] and angles [°]: Zn1–O1 1.935(4), Zn1–N1 2.208(4), Zn1–N2 2.158(5), Zn1–N3 1.945(4); O1–Zn1–N3 122.68(19), O1–Zn1–N2 96.26(18), N3–Zn1–N2 115.64(19), O1–Zn1–N1 93.54(17), N3–Zn1–N1 116.93(19), N2–Zn1–N1 108.09(17).

coordinated by three heteroatom donors of the tridentate ligand and one bis(trimethylsilyl)amido group in a distorted tetrahedral geometry. In contrast to the iminophenolate analogues,[62] the R_a configuration of the binaphthyl moiety in the ligand leads exclusively to the *R* configuration of the magnesium center, and the S_a configuration to the *S* configuration. The Mg1–N2 [2.202(2) Å] and Mg1–N3 [2.034(2) Å] bond lengths in complex **5a** are comparable to those in the iminophenolate magnesium analogue bearing the same substituents on the phenoxide ring [**4a** in ref.[62], 2.243(6) Å, 2.008(5) Å]. The corresponding angles around the metal center vary to a great extent in comparison to those in the ref.[62]. Moreover, widening of the dihedral angle of the binaphthyl moiety in **5a** [79.2(7)° vs. 75.7(4) in ref.[62]] is also observed. All these features suggest that the variation of the ligand skeleton from iminophenolate to aminophenolate does have a significant impact on the structural parameters of the complex.

As depicted in Figures 2, 3, and 4, zinc complexes **1b**, **3b**, and **5b** are also four-coordinate with three heteroatom donors of the tridentate ligand and one bis(trimethylsilyl)amido group,

in contast to the binaphthyl-based iminophenolate zinc analogue, in which the NMe_2 group of the iminophenolate ligand is not coordinated to zinc center even in the solid state.[62] Moreover, in comparison with the three-coordinate iminophenolate zinc analogue, the corresponding bond lengths between the zinc center and the central nitrogen atom in complexes **1b**, **3b**, and **5b** are somewhat elongated [2.152–2.206 Å vs. 1.969(2) Å], as are the bond lengths between the zinc center and the silylamido nitrogen atom [1.933–1.945 Å vs. 1.861(2) Å]. The dihedral angles of the biphenyl or binaphthyl moiety are 70.1(1), 76.0(4), and 78.1(6)° for **1b**, **3b**, and **5b** respectively, and are closely related with the rotational hindrance of the backbone moiety. Similar to magnesium complex **5a**, the R_a configuration of the biphenyl or binaphthyl moiety in the ligand leads to the *R* configuration of the zinc center, and the S_a configuration leads to the *S* configuration.

Ring-Opening Polymerization of *rac*-Lactide

All of the magnesium complexes **1a**–**5a** and zinc complexes **1b**, **3b**, **5b** are capable of initiating the ROP of *rac*-LA in the presence/absence of 2-propanol, producing PLAs with high molecular weights and relatively broad molecular weight distributions (M_w/M_n = 1.16–1.74) in both THF and toluene. Representative polymerization data are summarized in Table 2.

Compared with the previously reported biphenyl- or binaphthyl-based iminophenolate magnesium analogues, the activities of this series of magnesium complexes are significantly improved. At 50 °C in toluene, 200 equiv. of lactide monomer could be converted within 40–60 min by magnesium complexes **1a**–**5a**, while ca. 120–300 min were need to convert the same amount of monomer by the iminophenolate magnesium analogues at 50 °C or 70 °C.[61,62] This is a general trend for metal complexes bearing aminophenolate versus iminophenolate ligands.[65–68]

As depicted in Table 2, the backbone of the ancillary ligand has a remarkable influence on the catalytic activity of these magnesium complexes. In toluene, binaphthyl-based aminophenolate magnesium complex **5a** with *o*,*p*-cumyl groups on the phenolate ring exhibits higher catalytic activity than biphenyl-based magnesium complexes **1a** and **3a** with the same substituents on the phenolate ring; moreover, complex **1a** shows slightly higher activity than complex **3a** with two additional methyl groups substituting the biphenyl backbone. For example, complex **5a** achieves 94 % monomer conversion within 30 min in the presence of 2-propanol in toluene at room temp. (Run 19), whereas complexes **1a** and **3a** are less active. High monomer conversions are achieved within 60 min for **1a** (Run 3, 99 %) and within 90 min for **3a** (Run 11, 95 %) under identical conditions. However, this activity order is reversed in

Table 2. ROP of *rac*-LA initiated by magnesium and zinc complexes.

Run	Cat.	$[LA]_0/[M]_0/[i\text{PrOH}]$[a]	Solvent	*T* [°C]	*t* [min]	Conversion[b] [%]	$M_{n,calcd.}$[c] (10^4)	M_n[d] (10^4)	M_w/M_n[d]	P_r[e]
1	**1a**	200:1:0	toluene	25	930	28	–	–	–	–
2		200:1:0	toluene	50	60	90	2.59	4.50	1.40	0.49
3		200:1:1	toluene	25	60	99	2.85	2.36	1.38	0.47
4		200:1:0	thf	25	30	88	2.53	10.9	1.62	0.66
5		200:1:1	thf	25	10	89	2.76	4.24	1.66	0.69
6	**2a**	200:1:0	toluene	50	40	87	2.51	1.38	1.55	0.47
7		200:1:1	toluene	25	20	97	2.79	1.76	1.48	0.45
8		200:1:0	thf	25	20	88	2.53	1.90	1.50	0.58
9		200:1:1	thf	25	10	92	2.65	2.33	1.52	0.62
10	**3a**	200:1:0	toluene	50	60	89	2.56	2.17	1.53	0.51
11		200:1:1	toluene	25	90	95	2.74	1.93	1.44	0.53
12		200:1:0	thf	25	30	90	2.59	2.12	1.64	0.65
13		200:1:1	thf	25	10	91	2.62	2.25	1.68	0.65
14	**4a**	200:1:0	toluene	50	40	84	2.42	1.51	1.56	0.47
15		200:1:1	toluene	25	20	85	2.45	1.69	1.56	0.47
16		200:1:0	thf	25	20	94	2.71	3.20	1.74	0.60
17		200:1:1	thf	25	10	93	2.68	2.54	1.40	0.60
18	**5a**	200:1:0	toluene	50	40	85	2.45	4.64	1.42	0.51
19		200:1:1	toluene	25	30	94	2.71	3.21	1.41	0.49
20		200:1:0	thf	25	30	85	2.45	9.30	1.54	0.65
21		200:1:1	thf	25	20	98	2.82	2.53	1.42	0.62
22	**1b**	200:1:0	toluene	50	300	86	2.48	2.16	1.55	0.53
23		200:1:1	toluene	25	180	87	2.51	2.41	1.43	0.51
24		200:1:0	thf	25	480	85	2.45	5.00	1.57	0.58
25		200:1:1	thf	25	30	85	2.45	2.09	1.43	0.57
26	**3b**	200:1:0	toluene	50	300	76	2.19	4.13	1.51	0.49
27		200:1:1	toluene	25	240	92	2.65	1.98	1.35	0.47
28		200:1:0	thf	25	480	82	2.36	3.89	1.55	0.58
29		200:1:1	thf	25	30	80	2.30	1.75	1.39	0.56
30	**5b**	200:1:0	toluene	50	300	91	2.62	3.42	1.62	0.53
31		200:1:1	toluene	25	180	97	2.79	1.93	1.59	0.53
32		200:1:0	thf	25	420	71	2.04	12.2	1.45	0.58
33		200:1:1	thf	25	40	96	2.76	3.36	1.16	0.55

[a] $[rac\text{-LA}]_0$ = 1.0 M, $[M]_0$ = 0.005 M. [b] Determined by ^{1}H NMR spectroscopy. [c] $M_{n,calcd.} = ([rac\text{-LA}]_0/[M]_0) \times 144.13 \times$ % conversion. [d] Determined by GPC, Waters M515 pump, 25 °C, 1 mL min^{-1}, PS standards. [e] Probability of forming a new *r* diad, determined by homonuclear-decoupled ^{1}H NMR spectroscopy.

THF, in which complex **3a** is the most active catalyst. It seems that the influence of the ligand backbone is predominantly electronic rather than steric. In toluene, the electron-withdrawing effect of the backbone may increase the Lewis acidity of the metal center, which is favorable for the coordination of monomer and therefore enhancement of the activity. However, in THF, the solvent molecules compete with the monomer to coordinate to the magnesium center. In this case, the increase in Lewis acidity would make the competition more serious, and thereby lead to a decrease in activity.

Besides the ligand backbone, the substituents, particularly that at the *ortho* position of the phenoxide unit, also play an important role in determining the catalytic activity. Magnesium complexes bearing an *o*-trityl substituent on the phenolate ring display higher catalytic activity than those with an *o*-cumyl substituent.[61] By using complex **1a** with an *o*-cumyl substituent as the initiator, a monomer conversion of 99 % can be achieved within 60 min at room temp. (Run 3), whereas complex **2a** with a sterically bulkier *o*-trityl group gives 97 % conversion within 20 min under otherwise the same conditions (Run 7). Similarly, complex **4a** also exhibits higher catalytic activity than complex **3a**. Likely, the introduction of sterically bulkier groups, especially at the *ortho* position of the phenoxide oxygen atom, might protect more efficiently the active metal center from aggregation and therefore lead to an increase in activity, as is observed for most of the reported catalyst systems.[69,70]

In our previous work,[61,70] when the polymerization was carried out in THF, a significant enhancement of the activity toward *rac*-LA polymerization was observed for magnesium complexes bearing biphenyl-based iminophenolate ligands, especially for those bearing *o*-trityl-substituted ligands (monomer conversions up to 94 % within 1.5–2 min in THF at room temp. vs. 93–95 % within 120 min in toluene at 70 °C). Moreover, the addition of 2-propanol led to a remarkable decrease of the catalytic activity in THF.[61] However, the enhancement of the activity is not so apparent for the binaphthyl-based iminophenolate magnesium complexes, and the addition of 2-propanol to the polymerization mixture in THF also has no obvious influence on the activity of these complexes.[62] Such trends are quite abnormal, and are observed neither for most of the magnesium and zinc complexes reported in literature[35,71,72] nor for magnesium complexes **1a**–**5a** in this work. Therefore, we hypothesize that the aminophenolate ligand framework may lead to some different structural features to complexes **1a**–**5a** in solution compared with their biphenyl- or binaphthyl-based iminophenolate analogues. To prove this assumption, 2 equiv. of thf were added to a solution of complex **2a** in C_6D_6 and the mixture was monitored by ^{1}H NMR spectroscopy. Two sets of resonances could be identified in the ^{1}H NMR spectrum. One belongs to complex **2a** (ca. 60 %), and the other set could be assigned to a new structure with a dissociated NMe_2 group, since only one singlet is found for the NMe_2 group (see Figure S1). The ratio of these two structures remains constant on standing overnight at ambient temperature. On increasing the amount of thf to about 4 equiv., the percentage of the new species increases to about 90 % and a small amount of complex **2a** is still detectable (see Figure S2). Nevertheless, easy dissociation of the NMe_2 group in biphenyl-based iminophenolate magnesium complex could be observed on treatment with 2 equiv. of thf, and the binaphthyl-based iminophenolate magnesium analogue exits with a dissociated NMe_2 group even in C_6D_6.[61,62] These results indicate clearly stronger coordination of the NMe_2 group to the magnesium center in **2a** relative to the iminophenolate analogues, and this is then suggested to be a crucial factor leading to the above-mentioned discrepancy between the polymerization behaviors of these two systems. Notably, the competition for coordination to the metal center between the NMe_2 group and monomer still exists, although the NMe_2 group completely dissociates from the metal center in THF, which decreases the catalytic activity to some extent.

Compared with magnesium complexes **1a**–**5a**, zinc complexes **1b**, **3b**, and **5b** show significantly lower catalytic activities toward the ROP of *rac*-LA in both solvents. This is normal but in contrast to our previous report on the binaphthyl-based iminophenolate analogue, in which the three-coordinate zinc complex shows higher activity than the corresponding magnesium complex in toluene.[62] We attribute this difference to the stable coordination of the NMe_2 group to the zinc center in **1b**, **3b**, and **5b**. When a solution of typical zinc complex **1b** in C_6D_6 was treated with 1 equiv. of thf, the ^{1}H NMR spectrum showed that all the resonances remained unchanged (see Figure S3). It is conceivable that, for this series of complexes, the interaction of the NMe_2 group with the zinc center may be stronger and less influenced by thf, which accounts for the normal activity trend observed for these complexes.

As shown in Table 2, in contrast to the magnesium complexes, the variation of the ligand backbone leads to the same activity order of **5b** > **1b** ≥ **3b** in both solvents. Probably it is related to the difference in Lewis acidity between the two elements. Moreover, zinc complexes also show increased activities in thf and in the presence of alcohol.

The PLAs produced by magnesium and zinc silylamido complexes have broad polydispersities (M_w/M_n = 1.40–1.74) and M_n values that are smaller or larger than the theoretical ones. Two possibilities are normally suggested to account for this: the use of a metal silylamide as the initiator, which is known to be less nucleophilic than alkoxides, leads to relatively slow initiation with respect to chain propagation; and inter-/intramolecular transesterification takes place as a side reaction resulting in the formation of macrocycles and chains with a broad molecular weight distribution. Even in the presence of 2-propanol, the obtained PLAs still have broad molecular weight distributions (M_w/M_n = 1.16–1.59), and in most of the cases the M_n values are slightly lower than the theoretical ones. All these results indicate that the ROP of *rac*-LA by these magnesium and zinc complexes is not well controlled and may have involved transesterification to a considerable extent.

The initiation mechanism with the addition of 2-propanol was investigated by monitoring the NMR-scale reaction of complex **1a** and 2-propanol (1:1) in C_6D_6. Free $HN(SiMe_3)_2$ was released quantitatively (δ = 0.09 ppm); neither free proligand **L^{1}H** nor 2-propanol could be observed in the ^{1}H NMR spectrum. All these features support the generation of the magnesium isopropoxide species "[L^{1}MgO*i*Pr]", probably in aggregated form

(see Figure S4). On further addition of 20 equiv. of *rac*-LA to the above C_6D_6 solution, the active oligomer was produced within a short period according to the assignments reported in literature.[62,70] The ^{1}H NMR spectrum indicated that the NMe_2 group was dissociated from the active metal center, since only one singlet was displayed at δ = 2.48 ppm (see Figure S5).

On the basis of these results, kinetic studies on *rac*-LA polymerization were carried out in toluene. For $[LA]_0$ = 1.0 M and [**1a**] = [*i*PrOH] = 5.0, 3.3, 2.5, 2 mM, a linear relationship between $\ln([LA]_0/[LA]_t)$ and time can be observed (see Figure S6). The plot of k_{app} versus [**1a**] also has a linear relationship (see Figure S7). The polymerization shows first-order dependence on both monomer and initiator concentrations, which further implies that the concentration of active species remains unchanged during the entire polymerization, although transesterification reactions occur.

The ^{1}H NMR spectrum indicates that the purified oligomer (obtained with $[rac\text{-LA}]_0/[\mathbf{1a}]_0/[i\text{PrOH}]_0$ = 20:1:1) is capped by an isopropyl ester and a hydroxyl group on the two chain ends (see Figure S8). The ESI-TOF mass spectrum of the same sample exhibits a series of peaks with *m*/*z* of 72*n* + 60 (*i*PrOH) + 23 (Na^+) (see Figure S9), which further confirms the above conclusion. It is therefore suggested that the magnesium isopropoxide species "[L^{1}MgO*i*Pr]" generated in situ by the reaction of the metal silylamido complex **1a** and 2-propanol initiates the polymerization of *rac*-LA by a coordination/insertion mechanism, which leads to the formation of linear PLAs with isopropyl ester and hydroxyl termini.

All the magnesium and zinc silylamido complexes exhibit atactic selectivity in toluene and a certain heteroselectivity in THF. Compared with the biphenyl- or binaphthyl-based iminophenolate analogues, the heteroselectivities of magnesium complexes **1a**–**5a** are slightly lower (P_r = 0.58–0.69 vs. 0.67–0.77),[61,62] but the heteroselectivities of zinc complexes **1b**, **3b**, and **5b** are notably lower (P_r = 0.55–0.58 vs. 0.80–0.83).[62] This may also be related to the stronger coordination of the NMe_2 group to the metal center in the aminophenolate complexes of this work. The influence of the ligand backbone on the stereoselectivity of the corresponding complexes is not conclusive, whereby magnesium complexes **1a**, **3a** and **5a** with *o*,*p*-cumyl substituents on the phenolate ring show slightly higher preference for heterotactic dyad enchainment.

Ring-Opening Polymerization of α-MeTMC

This series of magnesium and zinc complexes also proved to be active initiators for the ROP of α-MeTMC in toluene at room temperature, and gave poly(α-MeTMC)s with high molecular weights and moderate to high regioselectivities.

As shown in Table 3, the magnesium complexes **1a**–**5a** are highly active toward α-MeTMC polymerization as single-component initiators in toluene at room temperature. The structure of the ancillary ligand has a significant influence on the catalytic activity. Magnesium complexes with an *o*-trityl substituent on the phenolate ring show remarkably higher catalytic activity than those with an *o*-cumyl substituent. For example, magnesium complex **4a** with an *o*-trityl substituent can effectively polymerize 200 equiv. of α-MeTMC at room temperature, and a monomer conversion of 93 % could be achieved within 5 min (Table 3, Run 4), whereas the monomer conversion is 91 % within 40 min for complex **3a** with an *o*-cumyl substituent (Table 3, Run 3). In addition, the introduction of two methyl groups in the biphenyl skeleton decreases the catalytic activity of complex **3a** to a great extent. With complex **1a** as the initiator, a conversion of 92 % can be reached within 10 min in toluene, whereas complex **3a** shows much lower activity in toluene with a monomer conversion of up to 91 % in 40 min. Such an influence is not observed for complex **4a** with an *o*-trityl-substituted ligand. Moreover, the activity order of **1a** > **5a** > **3a** for magnesium complexes with *o*,*p*-cumyl substituents on the phenolate ring implies that the influence of the ligand backbone may be both electronic and steric, whereby the electron-withdrawing effect is beneficial, and steric bulk is unfavorable.

Compared with the previously reported iminophenolate magnesium analogues,[61,62] the activities of magnesium complexes **1a**–**5a** are significantly improved relative to those of the biphenyl-based series (conversion of 85–95 % within 5–40 min at room temp. vs. 90–95 % within 60–180 min at 70 °C), but are comparable to those of the binaphthyl-based analogues (conversion of 91–94 % within 10–20 min). It seems that the variation of the ligand framework from iminophenolate to aminophenolate is more favorable for the biphenyl-based system. Such a variation may enhance the electrophilicity of the metal center and thereby increase the catalytic activity. In the binaphthyl-based system, the increase in steric bulk of the ligand may

Table 3. ROP of racemic α-MeTMC initiated by magnesium and zinc complexes in toluene.[a]

Run	Cat.	$[\alpha\text{-MeTMC}]_0/[M]_0/[i\text{PrOH}]$	*t* [min]	Conversion[b] [%]	$M_{n,calcd.}$[c] (10^4)	M_n[d] (10^4)	M_w/M_n[d]	X_{reg}[e]	T_g[f] [°C]
1	**1a**	200:1:0	10	92	2.13	7.92	1.74	0.81	7.83
2	**2a**	200:1:0	5	94	2.18	6.25	2.05	0.90	10.87
3	**3a**	200:1:0	40	91	2.11	6.35	1.64	0.88	10.54
4	**4a**	200:1:0	5	93	2.16	7.36	1.99	0.93	9.18
5	**5a**	200:1:0	10	85	1.97	6.47	1.67	0.89	10.87
6	**1b**	200:1:0	150	92	2.13	6.94	1.75	0.83	10.87
7	**1b**	200:1:1	120	92	2.13	5.23	1.34	0.81	9.84
8	**3b**	200:1:0	300	90	2.09	7.87	1.61	0.82	8.48
9	**3b**	200:1:1	180	91	2.11	5.99	1.44	0.82	10.54
10	**5b**	200:1:0	180	95	2.20	8.07	1.75	0.83	10.22
11	**5b**	200:1:1	120	90	2.09	5.55	1.41	0.83	8.47

[a] : $[\alpha\text{-MeTMC}]_0$ = 1.0 M; in toluene, at 25 °C. [b] Determined by ^{1}H NMR spectroscopy. [c] $M_{n,calcd.} = ([\alpha\text{-MeTMC}]_0/[M]_0) \times 116.05 \times$ % conversion. [d] Determined by GPC. [e] X_{reg} is the percentage of head-to-tail/tail-to-head linkages in the polymer chain, determined by ^{13}C NMR spectroscopy. [f] Determined by DSC.

counteract the positive electronic influence arising from such a framework variation, and no obvious change of the activity occurs.

Similar to the trend observed for *rac*-LA polymerization, zinc complexes **1b**, **3b**, and **5b** exhibit significantly lower catalytic activity in comparison with magnesium complexes. Two to six hours were needed for the zinc complexes to convert 200 equiv. of monomer to high conversions of 90–95 %, whereas high monomer conversions could be achieved by the corresponding magnesium complexes after 5–40 min under otherwise the identical conditions. Since only one zinc complex was obtained previously,[62] a thorough comparison between the iminophenolate and the aminophenolate systems is impossible. The higher activity of the binaphthyl-based iminophenolate zinc complex compared to complex **5b** suggests that a similar trend to that found for magnesium complexes may also hold.

The influence of the ligand backbone on the activity of these zinc complexes is similar to that of the magnesium complexes, with an activity order of **1b** > **5b** > **3b**. For instance, with biphenyl-based zinc complex **1b** as the initiator, a monomer conversion of 92 % can be reached within 150 min (Table 3, Run 6); binaphthyl-based zinc complex **5b** gives 95 % monomer conversion within 180 min under otherwise the same conditions (Table 3, Run 10), whereas complex **3b** shows the lowest activity among them, and only gives 90 % conversion within 300 min (Table 3, Run 8).

Compared with zinc silylamido complexes, the of zinc complex/2-propanol systems **1b**/, **3b**/, and **5b**/2-propanol exhibit higher catalytic activity for the polymerization of α-MeTMC. For example, **3b**/2-propanol can convert 91 % of lactide monomer to PLA within 180 min in toluene (Table 3, Run 9), whereas the yield is only 90 % after 300 min with complex **3b** alone (Table 3, Run 8). The same trend is also found for zinc complexes **1b** and **5b**.

To better understand the polymerization mechanism of α-MeTMC, the ^{1}H NMR spectrum of a purified oligomer sample prepared with $[\alpha\text{-MeTMC}]_0/[\mathbf{1b}]_0/[i\text{PrOH}]_0$ = 20:1:1 was determined. The resonances at δ = 1.22 ppm and 4.98 ppm can be ascibed to the $-OCH(CH_3)_2$ end group, while the resonances at 4.36, 3.68, 1.28 ppm are characteristic peaks of the other chain terminus [$-OCH_2CH_2CH(CH_3)OH$] (see Figure S10). All these features indicate that the polymer is end-capped with hydroxyl and isopropyl ester groups,[61,62] which were further comfirmed by ESI-TOF mass spectrometry (Figure S11). Likely due to enhanced transesterification reactions, oligomers end-capped with isopropyl group on both ends are also detected.

According to the literature,[60] microstructures of typical poly(α-MeTMC)s were analyzed by ^{13}C NMR spectroscopy. Four signals at 154.88, 154.4, 154.01, and 153.95 ppm can be observed, which are assigned to carbonyl groups of different environments [O–C(O)]. The regioselectivity of a given complex toward α-MeTMC polymerization can be obtained by calculating the relative intensity of the resonance at δ = 154.4 ppm in the total carbonyl region. As shown in Table 3, magnesium complex **4a** exhibits the highest regioselectivity (X_{reg} = 0.93) among these magnesium and zinc complexes (X_{reg} = 0.81–0.90; see Figure S12), and it is also the most regioselective magnesium initiator reported to date. Both the substituents and the ligand backbone exert a remarkable influence on the regioselectivity of these complexes. The introduction of an *o*-trityl group in the aminophenolate ligands leads to magnesium complexes showing higher regioselectivity. The selectivity order of **1a** < **3a** < **5a** indicates that the backbone of the ligand influences the regioselectivity of the corresponding magnesium complex sterically. The same order is also valid for the zinc complexes.

The regioselectivities of this series of magnesium complexes toward α-MeTMC polymerization are generally higher than those of the related iminophenolate magnesium analogues, while a reverse trend is observed for zinc complexes. A high regioselectivity of 0.98 was previously achieved by the binaphthyl-based iminophenolate zinc complex,[62] whereas the regioselectivities of zinc complexes **1b**, **3b**, and **5b** are obviously lower (X_{reg} = 0.81–0.83). It is conceivable that the increased steric bulk of these aminophenolate ligands relative to their iminophenolate counterparts are beneficial for the magnesium center but not for the zinc center toward the regioselective polymerization of α-MeTMC.

Moreover, although the regioselectivities of these complexes vary to some extent, the glass transition temperatures T_g of the resultant polymers are quite similar (Table 3). Similar to our previous work, no obvious relationship could be established between the regioregularity and the T_g value.

Conclusions

Several monomeric magnesium and zinc complexes derived from biphenyl-or binaphthyl-based aminophenol proligands were synthesized. X-ray diffraction studies demonstrated that both magnesium complex **5a** and zinc complexes **1b**, **3b**, **5b** have a four-coordinate metal center in the solid state. All complexes efficiently catalyzed the polymerization of *rac*-LA and racemic α-MeTMC under mild conditions. For *rac*-LA polymerization, the catalytic activity order is Mg > Zn, and all complexes are more active in the presence of 2-propanol and in thf. The structure of the ancillary ligand has a remarkable impact on the catalytic behavior of the corresponding complex. Among them, biphenyl-based magnesium complex **2a** with an *o*-trityl group on the phenolate ring is most active, and magnesium complex **1a** bearing a ligand with the same backbone but an *o*-cumyl group is the most heteroselective (P_r = 0.69). For α-MeTMC polymerization, magnesium complexes are significantly more active than zinc complexes in toluene. Magnesium complexes **2a** and **4a** with an *o*-trityl group exhibit higher activity than the other complexes. These complexes display moderate to high regioselectivity, and the highest value (X_{reg} = 0.93) is obtained with magnesium complex **4a**.

Experimental Section

Materials and Methods: All manipulations were performed under a dry argon atmosphere by using standard Schlenk-line or glovebox techniques. Toluene and *n*-hexane were heated to reflux over

sodium benzophenone ketyl prior to use. [D_6]Benzene was carefully dried and stored in the glove box. Mg[$N(SiMe_3)_2]_2$,[73] Zn[$N(SiMe_3)_2]_2$,[74] 2-bromomethyl-4,6-dicumylphenol,[75] and 2-bromomethyl-4-methyl-6-tritylphenol[75] were synthesized according to literature methods. Racemic 4-methyl-1,3-dioxan-2-one (α-methyltrimethylene carbonate, α-MeTMC) was synthesized by following a literature procedure.[58] *rac*-LA (Aldrich) was recrystallized from dry toluene and then sublimed twice under vacuum at 80 °C. 2-Propanol was dried with calcium hydride prior to distillation. All other chemicals were commercially available and used after appropriate purification. Glassware and vials used in the polymerization were dried in an oven at 120 °C overnight and exposed to a vacuum/argon cycle three times.

NMR spectra were recorded with Bruker AVANCE 400 and Varian 300 spectrometers at 25 °C (^{1}H: 300 MHz, 400 MHz; ^{13}C: 100 MHz) unless otherwise stated. Chemical shifts for ^{1}H and ^{13}C NMR spectra were referenced internally using the residual solvent resonances and reported relative to TMS. Elemental analyses were performed with an EA-1106 instrument. Spectroscopic analyses of polymers were performed in $CDCl_3$. Gel permeation chromatography (GPC) was carried out with a Waters 1515 Breeze instrument in thf at 35 °C, at a flow rate of 1 mL min^{-1}. Calibration standards were commercially available narrowly distributed linear polystyrene samples that cover a broad range of molar masses ($6 \times 10^3 < M_n < 6 \times 10^5$ g mol^{-1}). Differential scanning calorimetric (DSC) curves were taken with a PerkinElmer Pyris 1 instrument. All samples were cooled to −50 °C and heated to 60 °C for the first scan. After being kept for 3 min, they were again cooled to −50 °C, and heated to 60 °C for the second cycle. The heating rate was 10 °C min^{-1}.

2-{[*N*-ethyl-*N*-(2′-dimethylamino-1,1′-biphenyl-2-yl)amino]-methyl}-4,6-dicumylphenol (L^1H): A solution of 2-bromomethyl-4,6-dicumylphenol (3.39 g, 8.00 mmol) in dry thf (20 mL) was added to a stirred solution of *N*-ethyl-*N*′,*N*′-dimethyl-1,1′-biphenyl-2,2′-diamine (1.92 g, 8.00 mmol) in dry thf (15 mL), and then a solution of triethylamine (1.68 mL) in dry thf (5 mL) was added dropwise and a precipitate formed. The reaction mixture was stirred for 1 h. After filtration, the solvent of the filtrate was removed under vacuum to give a sticky solid. The crude product was purified by flash chromatography within several minutes on a 5 cm silica gel column (pretreated with NEt_3) with petroleum ether/ethyl acetate in gradient polarity as the eluent.[63] The pure product was obtained as an off-white solid (3.19 g, 68.4 %), m.p. 43–45 °C. ^{1}H NMR ($CDCl_3$, 400 MHz): δ = 8.90 (s, 1 H, ArOH), 7.32–7.22 (m, 8 H, ArH), 7.20–7.14 (m, 5 H, ArH), 7.12–7.05 (m, 3 H, ArH), 6.94 (d, J = 7.0 Hz, 1 H, ArH), 6.87 (t, J = 7.3 Hz, 1 H, ArH), 6.70–6.66 (m, 2 H, ArH), 3.94 (s, 2 H, ArCH_2), 2.62–2.44 (m, 2 H, NCH_2CH$_3$), 2.15 [s, 6 H, N$(CH_3)_2$], 1.66 [s, 6 H, C$(CH_3)_2$Ph], 1.53 [s, 6 H, C$(CH_3)_2$Ph], 0.53 (t, J = 6.8 Hz, 3 H, NCH$_2$CH_3) ppm. ^{13}C NMR ($CDCl_3$, 100 MHz): δ = 153.2, 151.6, 151.5, 150.8, 148.2, 139.7, 139.2, 134.6, 133.3, 132.2, 131.4, 128.1, 127.8, 127.4, 126.7, 125.8, 125.6, 125.3, 124.9, 124.5, 121.9, 121.1, 121.0, 118.5 (all Ar C), 59.2 (ArCH_2), 45.8 (NCH_2CH$_3$), 43.3 [N$(CH_3)_2$], 42.4 [*C*$(CH_3)_2$Ph], 41.8 [*C*$(CH_3)_2$Ph], 31.1 [C$(CH_3)_2$Ph], 30.2 [C$(CH_3)_2$Ph], 10.7 (NCH_2CH$_3$) ppm. $C_{41}H_{46}N_2O$ (582.83): calcd. C 84.49, H 7.96, N 4.81; found C 84.67, H 8.24, N 4.42.

2-{[*N*-ethyl-*N*-(2′-dimethylamino-1,1′-biphenyl-2-yl)amino]-methyl}-4-methyl-6-tritylphenol (L^2H): This compound was prepared in an analogous manner to that described for **L^1H**, except that 2-bromomethyl-4-methyl-6-tritylphenol (3.54 g, 8.00 mmol) was used to afford proligand **L^2H** as an off-white solid (3.33 g, 69.1 %), m.p. 165–168 °C. ^{1}H NMR ($CDCl_3$, 400 MHz): δ = 8.91 (s, 1 H, ArOH), 7.36–7.03 (m, 20 H, ArH), 6.94 (d, J = 7.1 Hz, 1 H, ArH), 6.86–6.81 (m, 2 H, ArH), 6.71 (s, 1 H, ArH), 6.57 (d, J = 8.2 Hz, 1 H, ArH), 3.99 (d, J = 13.4 Hz, 1 H, ArCH_2), 3.92 (d, J = 13.4 Hz, 1 H, ArCH_2), 2.56–2.31 (m, 2 H, NCH_2CH$_3$), 2.13 (s, 3 H, ArCH_3), 2.12 [s, 6 H, N$(CH_3)_2$], 0.49 (t, J = 7.0 Hz, 3 H, NCH$_2$CH_3) ppm. ^{13}C NMR ($CDCl_3$, 100 MHz): δ = 153.5, 150.8, 147.9, 146.1, 140.1, 133.5, 133.3, 132.4, 131.2, 130.1, 129.5, 128.8, 128.4, 127.9, 126.9, 126.2, 125.1, 122.2, 121.9, 121.1, 119.0 (all Ar C), 63.3 (ArCH_2), 59.7 (Ar*C*Ph$_3$), 45.1 (NCH_2CH$_3$), 43.5 [N$(CH_3)_2$], 21.0 (ArCH_3), 11.1 (NCH_2CH$_3$) ppm. $C_{43}H_{42}N_2O$ (602.82): calcd. C 85.68, H 7.02, N 4.65; found C 85.60, H 7.01, N 4.45.

2-{[*N*-ethyl-*N*-(2′-dimethylamino-6,6′-dimethyl-1,1′-biphenyl-2-yl)amino]methyl}-4,6-dicumyl-phenol (L^3H): This compound was prepared in an analogous manner to that described for **L^1H**, except that *N*-ethyl-*N*′,*N*′,6,6′-tetramethyl-1,1′-biphenyl-2,2′-diamine (2.15 g, 8.00 mmol) and 2-bromomethyl-4,6-dicumylphenol (3.39 g, 8.00 mmol) were used to afford proligand **L^3H** as an off-white solid (1.24 g, 25.3 %), m.p. 75–77 °C. ^{1}H NMR ($CDCl_3$, 300 MHz): δ = 8.85 (s, 1 H, ArOH), 7.36–7.21 (m, 5 H, ArH), 7.16 (dd, J = 9.0, 4.8 Hz, 5 H, ArH), 7.09 (t, J = 6.6 Hz, 5 H, ArH), 6.80 (d, J = 7.4 Hz, 1 H, ArH), 6.69 (s, 1 H, ArH), 6.58 (d, J = 8.2 Hz, 1 H, ArH), 3.93 (d, J = 13.4 Hz, 1 H, ArCH_2), 3.83 (d, J = 13.4 Hz, 1 H, ArCH_2), 2.62–2.43 (m, 2 H, NCH_2CH$_3$), 2.10 [s, 6 H, N$(CH_3)_2$], 2.02 (s, 3 H, ArCH_3), 1.87 (s, 3 H, ArCH_3), 1.76–1.59 [s, 6 H, C$(CH_3)_2$Ph], 1.55 [s, 3 H, C$(CH_3)_2$Ph], 1.49 [s, 3 H, C$(CH_3)_2$Ph], 0.57 (t, J = 7.0 Hz, 3 H, NCH$_2$CH_3) ppm. ^{13}C NMR ($CDCl_3$, 100 MHz): δ = 153.4, 151.6, 151.5, 150.8, 148.6, 138.9, 138.6, 137.8, 136.5, 134.4, 131.2, 127.7, 127.4, 127.3, 127.0, 126.7, 125.6, 125.5, 125.3, 124.3, 124.2, 123.5, 121.0, 120.4, 117.2 (all ArC), 59.7 (ArCH_2), 45.5 (NCH_2CH$_3$), 43.0 [N$(CH_3)_2$], 42.3 [*C*$(CH_3)_2$Ph], 41.7 [*C*$(CH_3)_2$Ph], 31.1 [C$(CH_3)_2$Ph], 30.7 [C$(CH_3)_2$Ph], 20.6 (ArCH_3), 19.9 (ArCH_3), 10.6 (NCH_2CH$_3$) ppm. $C_{43}H_{50}N_2O$ (610.88): calcd. C 84.55, H 8.25, N 4.59; found C 84.23, H 8.59, N 4.16.

2-{[*N*-ethyl-*N*-(2′-dimethylamino-6,6′-dimethyl-1,1′-biphenyl-2-yl)amino]methyl}-4-methyl-6-tritylphenol (L^4H): This compound was prepared in an analogous manner to that described for **L^1H**, except that *N*-ethyl-*N*′,*N*′,6,6′-tetramethylbiphenyl-2,2′-diamine (2.15 g, 8.00 mmol) and 2-bromomethyl-4-methyl-6-tritylphenol (3.54 g, 8.00 mmol) were used to afford proligand **L^4H** as an off-white solid (2.34 g, 69.6 %), m.p. 90–93 °C. ^{1}H NMR ($CDCl_3$, 400 MHz): δ = 8.76 (s, 1 H, ArOH), 7.29–7.22 (m, 1 H, ArH), 7.22–7.03 (m, 17 H, ArH), 6.92–6.83 (m, 2 H, ArH), 6.71 (s, 2 H, ArH), 6.47 (d, J = 8.1 Hz, 1 H, ArH), 4.02 (d, J = 13.6 Hz, 1 H, ArCH_2), 3.85 (d, J = 13.4 Hz, 1 H, ArCH_2), 2.49–2.28 (m, 2 H, NCH_2CH$_3$), 2.13 (s, 3 H, ArCH_3), 2.09 [s, 6 H, N$(CH_3)_2$], 1.98 (s, 3 H, ArCH_3), 1.83 (s, 3 H, ArCH_3), 0.46 (t, J = 7.0 Hz, 3 H, NCH$_2$CH_3) ppm. ^{13}C NMR ($CDCl_3$, 100 MHz): δ = 153.5, 150.6, 148.3, 146.0, 138.6, 137.9, 136.3, 133.2, 131.1, 131.0, 130.2, 128.5, 128.0, 127.4, 127.1, 126.7, 125.9, 124.9, 123.6, 122.2, 120.4, 117.3 (all Ar C), 63.1 (ArCH_2), 59.6 (Ar*C*Ph$_3$), 45.3 (NCH_2CH$_3$), 43.2 [N$(CH_3)_2$], 20.9 (ArCH_3), 20.6 (ArCH_3), 19.9 (ArCH_3), 11.0 (NCH_2CH$_3$) ppm. $C_{45}H_{46}N_2O$ (630.87): calcd. C 85.67, H 7.35, N 4.44; found C 85.17, H 7.02, N 4.62.

2-{[*N*-ethyl-*N*-(2′-dimethylamino-1,1′-binaphthyl-2-yl)amino]-methyl}-4,6-dicumylphenol (L^5H): This compound was prepared in an analogous manner to that described for **L^1H**, except that *N*-ethyl-*N*′,*N*′-dimethyl-1,1′-binaphthyl-2,2′-diamine (2.72 g, 8.00 mmol) and 2-bromomethyl-4,6-dicumylphenol (3.39 g, 8.00 mmol) were used to afford proligand **L^5H** as an off-white solid (4.74 g, 86.7 %), m.p. 165–167 °C. ^{1}H NMR ($CDCl_3$, 300 MHz): δ = 8.94 (s, 1 H, ArOH), 7.95 (d, J = 8.9 Hz, 1 H, ArH), 7.86 (d, J = 8.1 Hz, 1 H, ArH), 7.77 (dd, J = 8.5, 3.7 Hz, 2 H, ArH), 7.62 (d, J = 8.9 Hz, 1 H, ArH), 7.39 (dt, J = 8.1, 3.7 Hz, 1 H, ArH), 7.31–7.14 (m, 10 H, ArH), 7.05 (m, 6 H, ArH), 6.76 (d, J = 8.5 Hz, 1 H, ArH), 6.66 (d, J = 1.8 Hz, 1 H, ArH), 4.08 (d, J = 13.1 Hz, 1 H, ArCH_2), 3.85 (d, J = 13.1 Hz, 1 H, ArCH_2), 2.49 (q, J = 7.1 Hz, 2 H, NCH_2CH$_3$), 2.10 [s, 6 H, N$(CH_3)_2$],

1.64 [s, 6 H, C(CH_3)$_2$Ph], 1.45 [s, 6 H, C(CH_3)$_2$Ph], 0.38 (t, J = 7.1 Hz, 3 H, NCH$_2$$CH_3$) ppm. ^{13}C NMR ($CDCl_3$, 100 MHz): δ = 153.2, 151.6, 151.5, 149.7, 146.3, 139.0, 134.8, 134.5, 133.8, 133.5, 131.7, 129.4, 128.8, 128.8, 127.8, 127.8, 127.5, 127.3, 126.7, 126.2, 125.6, 125.5, 125.3, 125.2, 124.4, 124.2, 123.0, 122.9, 121.7, 120.8, 120.3 (all Ar C), 60.1 (ArCH_2), 46.0 (NCH_2CH$_3$), 43.1 [N(CH_3)$_2$], 42.4 [C(CH_3)$_2$Ph], 41.7 [C(CH_3)$_2$Ph], 31.1 [C(CH_3)$_2$Ph], 30.9 [C(CH_3)$_2$Ph], 11.5 (NCH$_2$$CH_3$) ppm. $C_{49}H_{50}N_2O$ (682.95): calcd. C 86.18, H 7.38, N 4.10; found C 85.63, H 7.41, N 3.90.

[(L^1)MgN(SiMe$_3$)$_2$] (1a): The proligand **L^{1}H** (0.583 g, 1.00 mmol) was added slowly to a solution of Mg[N(SiMe$_3$)$_2$]$_2$ (0.345 g, 1.00 mmol) in toluene (15 mL). The solution was stirred overnight at room temp. The resultant solution was filtered to remove a trace amount of impurities and the solvents evaporated to dryness under vacuum for several hours to give a foamlike material. Recrystallization from toluene/hexane afforded colorless crystals of complex **1a** (212 mg, 27.7 %), m.p. 166–167 °C. ^{1}H NMR (C_6D_6, 400 MHz): δ = 7.62 (s, 1 H, ArH), 7.47 (d, J = 7.8 Hz, 2 H, ArH), 7.28 (t, J = 7.7 Hz, 2 H, ArH), 7.19 (d, J = 8.3 Hz, 1 H, ArH), 7.14–7.09 (m, 1 H, ArH), 7.06 (d, J = 7.4 Hz, 2 H, ArH), 7.00 (d, J = 2.4 Hz, 1 H, ArH), 6.97–6.91 (m, 2 H, ArH), 6.81 (m, 5 H, ArH), 6.67 (d, J = 8.3 Hz, 1 H, ArH), 6.60 (d, J = 7.5 Hz, 1 H, ArH), 6.44 (d, J = 7.5 Hz, 1 H, ArH), 4.43 (d, J = 15.0 Hz, 1 H, ArCH_2), 3.85 (d, J = 15.1 Hz, 1 H, ArCH_2), 3.05–2.92 (m, 1 H, NCH_2CH$_3$), 2.84–2.72 (m, 1 H, CH_2CH$_3$), 2.46 [s, 3 H, N(CH_3)$_2$], 2.17 [s, 3 H, C(CH_3)$_2$Ph], 1.82 [s, 3 H, C(CH_3)$_2$Ph], 1.81 [s, 3 H, C(CH_3)$_2$Ph], 1.60 [s, 3 H, N(CH_3)$_2$], 1.31 [s, 3 H, C(CH_3)$_2$Ph], 0.42 [br. s, 9 H, Si(CH_3)$_3$], 0.29 (t, J = 6.9 Hz, 3 H, NCH$_2$$CH_3$), –0.01 [br. s, 9 H, Si(CH_3)$_3$] ppm. ^{13}C NMR (C_6D_6, 100 MHz): δ = 162.5, 154.2, 153.5, 146.2, 141.0, 136.6, 136.3, 135.0, 134.8, 134.2, 134.0, 129.6, 129.5, 128.2, 127.3, 127.3, 127.0, 126.2, 126.1, 126.0, 125.7, 125.6, 124.2, 122.4, 119.8 (all ArC), 57.4 (ArCH_2), 51.5 (NCH_2CH$_3$), 47.4 [N(CH_3)$_2$], 44.2 [N(CH_3)$_2$], 42.8 [C(CH_3)$_2$Ph], 42.6 [C(CH_3)$_2$Ph], 31.7 [C(CH_3)$_2$Ph], 31.5 [C(CH_3)$_2$Ph], 27.1 (NCH$_2$$CH_3$), 6.2 (Si$CH_3$) ppm. $C_{47}H_{63}MgN_3OSi_2$ (766.51): calcd. C 73.65, H 8.28, N 5.48; found C 73.50, H 8.27, N 5.24.

[(L^2)MgN(SiMe$_3$)$_2$] (2a): A similar method was employed to that described for **1a**. **L^{2}H** (0.603 g, 1.00 mmol) was treated with Mg[N(SiMe$_3$)$_2$]$_2$ (0.345 g, 1.00 mmol) in toluene (15 mL) at room temp. to give a foamlike material. Recrystallization from toluene/hexane afforded colorless crystals of complex **2a** (202 mg, 25.7 %). Because **2a** is very air sensitive, a poor elemental analysis was obtained, m.p. 239–241 °C. ^{1}H NMR (C_6D_6, 400 MHz): δ = 7.38 (s, 1 H, ArH), 7.34–7.28 (m, 7 H, ArH), 7.02–6.88 (m, 10 H, ArH), 6.87–6.81 (m, 4 H, ArH), 6.66 (d, J = 8.1 Hz, 2 H, ArH), 6.50 (dd, J = 8.5, 2.0 Hz, 1 H, ArH), 4.54 (d, J = 15.9 Hz, 1 H, ArCH_2), 4.06 (d, J = 15.9 Hz, 1 H, ArCH_2), 3.20–3.10 (m, 1 H, NCH_2CH$_3$), 3.02–2.92 (m, 1 H, CH_2CH$_3$), 2.43 [s, 3 H, N(CH_3)$_2$], 2.27 (s, 3 H, ArCH_3), 1.67 [s, 3 H, N(CH_3)$_2$], 0.46 (t, J = 6.9 Hz, 3 H, NCH$_2$$CH_3$), –0.05 [s, 18 H, Si($CH_3$)$_3$] ppm. ^{13}C NMR ($C_6D_6$, 100 MHz): δ = 162.7, 147.6, 146.6, 141.6, 136.4, 135.8, 135.2, 135.1, 135.0, 133.0, 131.8, 129.6, 129.6, 127.3, 126.4, 126.3, 126.0, 125.0, 122.9, 121.1, 120.3 (all ArC), 64.0 (ArCH_2), 56.5 (ArCPh_3), 51.0 (NCH_2CH$_3$), 50.2 [N(CH_3)$_2$], 43.8 (ArCH_3), 21.2 (NCH$_2$$CH_3$), 6.0 (Si$CH_3$) ppm. $C_{49}H_{59}MgN_3OSi_2$ (786.50): calcd. C 74.83, H 7.56, N 5.34; found C 74.32, H 7.16, N 4.55.

[(L^3)MgN(SiMe$_3$)$_2$] (3a): A similar method was employed to that described for **1a**. **L^{3}H** (0.795 g, 1.00 mmol) was treated with Mg[N(SiMe$_3$)$_2$]$_2$ (0.345 g, 1.00 mmol) in toluene (15 mL) at room temp. to give a foamlike material. Recrystallization from toluene/hexane afforded colorless crystals of complex **3a** (542 mg, 68.3 %), m.p. 156–158 °C. ^{1}H NMR (C_6D_6, 400 MHz): δ = 7.58 (d, J = 2.0 Hz, 1 H, ArH), 7.48 (d, J = 8.0 Hz, 2 H, ArH), 7.29 (t, J = 7.7 Hz, 2 H, ArH), 7.11 (t, J = 7.2 Hz, 1 H, ArH), 7.04 (d, J = 8.0 Hz, 1 H, ArH), 6.99 (d, J = 2.4 Hz, 1 H, ArH), 6.96–6.93 (m, 3 H, ArH), 6.91 (d, J = 7.9 Hz, 1 H, ArH), 6.87–6.83 (m, 2 H, ArH), 6.81–6.71 (m, 3 H, ArH), 6.61 (d, J = 8.3 Hz, 1 H, ArH), 4.50 (d, J = 15.0 Hz, 1 H, ArCH_2), 3.91 (d, J = 15.1 Hz, 1 H, ArCH_2), 2.98–2.75 (m, 2 H, NCH_2CH$_3$), 2.48 [s, 3 H, N(CH_3)$_2$], 2.17 [s, 3 H, C(CH_3)$_2$Ph], 1.81 [s, 3 H, C(CH_3)$_2$Ph], 1.80 [s, 3 H, C(CH_3)$_2$Ph], 1.58 [s, 3 H, N(CH_3)$_2$], 1.33 (s, 3 H, ArCH_3), 1.31 [s, 3 H, C(CH_3)$_2$Ph], 1.30 (s, 3 H, ArCH_3), 0.48 (t, J = 6.9 Hz, 3 H, NCH$_2$$CH_3$), 0.39 [s, 9 H, Si($CH_3$)$_3$], –0.03 [s, 9 H, Si($CH_3$)$_3$] ppm. ^{13}C NMR ($C_6D_6$, 100 MHz): δ = 162.4, 154.4, 153.5, 146.3, 140.7, 140.3, 138.3, 135.9, 134.5, 133.9, 132.0, 129.6, 128.7, 128.5, 128.1, 127.9, 127.4, 126.7, 126.2, 126.1, 126.1, 125.6, 124.0, 122.8, 118.5 (all ArC), 57.5 (ArCH_2), 50.2 (NCH_2CH$_3$), 45.5 [N(CH_3)$_2$], 42.8 [C(CH_3)$_2$Ph], 42.6 [C(CH_3)$_2$Ph], 31.7 [C(CH_3)$_2$Ph], 31.5 [C(CH_3)$_2$Ph], 27.2 (NCH$_2$$CH_3$), 20.4 (Ar$CH_3$), 19.9 (Ar$CH_3$), 6.5 (Si$CH_3$) ppm. $C_{49}H_{67}MgN_3OSi_2$ (794.56): calcd. C 74.07, H 8.50, N 5.29; found C 73.51, H 8.63, N 4.80.

[(L^4)MgN(SiMe$_3$)$_2$] (4a): A similar method was employed to that described for **1a**. **L^{4}H** (0.631 g, 1.00 mmol) was treated with Mg[N(SiMe$_3$)$_2$]$_2$ (0.345 g, 1.00 mmol) in toluene (15 mL) at room temp. to give a foamlike material. Recrystallization from toluene/hexane afforded colorless crystals of complex **4a** (240 mg, 29.5 %). Because **4a** is very air sensitive, a poor elemental analysis was obtained, m.p. 184–186 °C. ^{1}H NMR (C_6D_6, 400 MHz): δ = 7.39 (d, J = 1.8 Hz, 1 H, ArH), 7.32 (d, J = 7.6 Hz, 6 H, ArH), 7.18 (d, J = 7.6 Hz, 1 H, ArH), 7.12 (d, J = 7.5 Hz, 1 H, ArH), 7.05 (d, J = 7.1 Hz, 1 H, ArH), 6.99 (t, J = 7.6 Hz, 5 H, ArH), 6.96–6.87 (m, 4 H, ArH), 6.84 (t, J = 7.0 Hz, 2 H, ArH), 6.79 (d, J = 7.2 Hz, 1 H, ArH), 6.61 (d, J = 8.2 Hz, 1 H, ArH), 4.54 (d, J = 15.7 Hz, 1 H, ArCH_2), 4.11 (d, J = 15.7 Hz, 1 H, ArCH_2), 3.06 (q, J = 7.0 Hz, 2 H, NCH_2CH$_3$), 2.46 [s, 3 H, N(CH_3)$_2$], 2.27 (s, 3 H, ArCH_3), 1.64 [s, 3 H, N(CH_3)$_2$], 1.39 (s, 3 H, ArCH_3), 1.37 (s, 3 H, ArCH_3), 0.68 (t, J = 7.0 Hz, 3 H, NCH$_2$$CH_3$), –0.07 [s, 18 H, Si($CH_3$)$_3$] ppm. ^{13}C NMR ($C_6D_6$, 100 MHz): δ = 162.6, 147.7, 146.7, 141.1, 140.9, 139.0, 137.8, 134.7, 134.3, 133.1, 132.6, 131.8, 129.9, 129.7, 129.3, 129.0, 128.9, 128.5, 127.3, 125.6, 125.5, 125.0, 123.2, 120.9, 118.9 (all Ar C), 64.0 (ArCH_2), 56.5 (ArCPh_3), 49.8 (NCH_2CH$_3$), 48.1 [N(CH_3)$_2$], 44.6 (ArCH_3), 21.4 (ArCH_3), 20.6 (ArCH_3), 20.1 (NCH$_2$$CH_3$), 6.3 (Si$CH_3$) ppm. $C_{51}H_{63}MgN_3OSi_2$ (814.56): calcd. C 75.20, H 7.80, N 5.16; found C 75.44, H 7.66, N 4.33.

[(L^5)MgN(SiMe$_3$)$_2$] (5a): A similar method was employed to that described for **1a**. **L^{5}H** (0.683 g, 1.00 mmol) was treated with Mg[N(SiMe$_3$)$_2$]$_2$ (0.345 g, 1.00 mmol) in toluene (15 mL) at room temp. to give a foamlike material. Recrystallization from toluene/hexane afforded colorless crystals of complex **5a** (392 mg, 45.2 %), m.p. 145–148 °C. ^{1}H NMR (C_6D_6, 400 MHz): δ = 7.62–7.48 (m, 8 H, ArH), 7.36 (t, J = 7.6 Hz, 2 H, ArH), 7.09–7.00 (m, 2 H, ArH), 6.94 (t, J = 7.5 Hz, 1 H, ArH), 6.79 (d, J = 7.6 Hz, 2 H, ArH), 6.71 (t, J = 7.6 Hz, 1 H, ArH), 6.59 (t, J = 7.1 Hz, 1 H, ArH), 6.37 (t, J = 7.1 Hz, 1 H, ArH), 6.25–6.17 (m, 4 H, ArH), 4.61 (d, J = 15.1 Hz, 1 H, ArCH_2), 4.02 (d, J = 15.1 Hz, 1 H, ArCH_2), 2.88–2.83 (m, 1 H, CH_2CH$_3$), 2.67–2.62 [m, 4 H, NCH_2CH$_3$ and N(CH_3)$_2$], 2.15 [s, 3 H, C(CH_3)$_2$Ph], 1.87 [s, 3 H, C(CH_3)$_2$Ph], 1.85 [s, 3 H, C(CH_3)$_2$Ph], 1.54 [s, 3 H, N(CH_3)$_2$], 1.35 [s, 3 H, C(CH_3)$_2$Ph], 0.41 [br. s, 12 H, NCH$_2$$CH_3$ and Si(CH_3)$_3$], –0.09 [s, 9 H, Si(CH_3)$_3$] ppm. ^{13}C NMR (C_6D_6, 100 MHz): δ = 162.5, 154.0, 153.5, 144.8, 140.8, 136.2, 135.8, 135.4, 134.3, 132.1, 131.8, 131.2, 129.6, 129.3, 129.3, 128.5, 128.2, 127.6, 127.5, 127.4, 126.9, 126.7, 126.6, 126.6, 126.32, 126.26, 125.90, 125.87, 125.80, 125.75, 125.6, 124.0, 122.7, 118.9 (all Ar C), 57.9 (ArCH_2), 50.3 (NCH_2CH$_3$), 46.1 [N(CH_3)$_2$], 45.1 [C(CH_3)$_2$Ph], 42.7 [C(CH_3)$_2$Ph], 31.8 [C(CH_3)$_2$Ph], 31.5 [C(CH_3)$_2$Ph], 27.3 (NCH$_2$$CH_3$), 6.9 (Si$CH_3$) ppm. $C_{55}H_{67}MgN_3OSi_2$ (866.63): calcd. C 76.23, H 7.79, N 4.85; found C 76.53, H 8.33, N 4.62.

[(L^1)ZnN(SiMe$_3$)$_2$] (1b): The proligand **L^{1}H** (0.583 g, 1.00 mmol) was added slowly to a solution of Zn[N(SiMe$_3$)$_2$]$_2$ (0.386 g, 1.0 mmol) in toluene (15 mL). The solution was stirred overnight at room temp.

The resultant solution was filtered to remove a trace amount of impurities and the solvent evaporated to dryness under vacuum for several hours to give a foamlike material. Recrystallization from toluene/hexane afforded colorless crystals of complex **1b** (235 mg, 29.1 %), m.p. 128–130 °C. ^{1}H NMR (C_6D_6, 400 MHz): δ = 7.62 (s, 1 H, ArH), 7.47 (d, J = 7.8 Hz, 2 H, ArH), 7.28 (t, J = 7.6 Hz, 2 H, ArH), 7.21 (d, J = 8.3 Hz, 1 H, ArH), 7.10–7.03 (m, 3 H, ArH), 7.06–6.90 (m, 3 H, ArH), 6.85–6.75 (m, 5 H, ArH), 6.70 (d, J = 8.2 Hz, 1 H, ArH), 6.64 (d, J = 7.5 Hz, 1 H, ArH), 6.50 (d, J = 7.6 Hz, 1 H, ArH), 4.58 (d, J = 14.9 Hz, 1 H, ArCH_2), 3.88 (d, J = 14.9 Hz, 1 H, ArCH_2), 3.14–3.03 (m, 1 H, NCH_2CH$_3$), 2.89–2.79 (m, 1 H, CH_2CH$_3$), 2.47 [s, 3 H, N(CH$_3$)$_2$], 2.16 [s, 3 H, C(CH_3)$_2$Ph], 1.82 [s, 3 H, C(CH_3)$_2$Ph], 1.81 [s, 3 H, C(CH_3)$_2$Ph], 1.60 [s, 3 H, N(CH$_3$)$_2$], 1.39 [s, 3 H, C(CH_3)$_2$Ph], 0.41 [s, 9 H, Si(CH$_3$)$_3$], 0.28 (t, J = 6.9 Hz, 3 H, NCH$_2$CH_3), –0.03 [s, 9 H, Si(CH$_3$)$_3$] ppm. ^{13}C NMR (C_6D_6, 100 MHz): δ = 163.0, 154.2, 153.5, 147.5, 141.7, 136.9, 136.7, 135.3, 134.6, 134.3, 134.2, 129.3, 129.2, 128.2, 127.3, 126.93, 126.88, 126.0, 126.0, 125.8, 125.7, 125.6, 124.1, 121.1, 119.5 (all ArC), 58.8 (ArCH_2), 52.8 (NCH_2CH$_3$), 48.2 [N(CH$_3$)$_2$], 46.5 [N(CH$_3$)$_2$], 42.8 [C(CH$_3$)$_2$Ph], 42.6 [C(CH$_3$)$_2$Ph], 31.7 [C(CH$_3$)$_2$Ph], 31.5 [C(CH$_3$)$_2$Ph], 27.2 (NCH$_2$CH_3), 6.1 (SiCH$_3$) ppm. $C_{47}H_{63}N_3OSi_2Zn$ (807.59): calcd. C 69.90, H 7.86, N 5.20; found C 69.87, H 7.90, N 5.09.

[(L^3)ZnN(SiMe$_3$)$_2$] (3b): A similar method was employed to that described for **1b**. **L^{3}H** (0.611 g, 1.00 mmol) was treated with Zn[N(SiMe$_3$)$_2$]$_2$ (0.386 g, 1.00 mmol) in toluene (15 mL) at room temp. to give a foamlike material. Recrystallization from toluene/hexane afforded colorless crystals of complex **3b** (596 mg, 71.4 %), m.p. 131–135 °C. ^{1}H NMR (C_6D_6, 300 MHz): δ = 7.58 (s, 1 H, ArH), 7.48 (d, J = 7.3 Hz, 2 H, ArH), 7.29 (t, J = 7.7 Hz, 2 H, ArH), 7.08 (m, 2 H, ArH), 6.97–6.90 (m, 4 H, ArH), 6.86 (t, J = 8.8 Hz, 3 H, ArH), 6.81–6.73 (m, 3 H, ArH), 6.63 (d, J = 8.2 Hz, 1 H, ArH), 4.63 (d, J = 14.9 Hz, 1 H, ArCH_2), 3.95 (d, J = 14.9 Hz, 1 H, ArCH_2), 3.08–3.02 (m, 1 H, CH_2CH$_3$), 2.90–2.80 (m, 1 H, NCH_2CH$_3$), 2.49 [s, 3 H, N(CH$_3$)$_2$], 2.16 [s, 3 H, C(CH_3)$_2$Ph], 1.82 [s, 3 H, C(CH_3)$_2$Ph], 1.81 [s, 3 H, C(CH_3)$_2$Ph], 1.58 [s, 3 H, N(CH$_3$)$_2$], 1.40 (s, 3 H, ArCH_3), 1.37 [s, 3 H, C(CH_3)$_2$Ph], 1.34 (s, 3 H, ArCH_3), 0.49 (t, J = 7.0 Hz, 3 H, NCH$_2$CH_3), 0.38 [s, 9 H, Si(CH$_3$)$_3$], –0.01 [s, 9 H, Si(CH$_3$)$_3$] ppm. ^{13}C NMR (C_6D_6, 100 MHz): δ = 162.8, 154.4, 153.5, 147.5, 141.1, 140.4, 138.3, 136.3, 134.7, 134.1, 132.3, 129.4, 129.0, 128.1, 127.4, 126.2, 126.0, 125.9, 125.6, 124.0, 121.5, 118.1 (all Ar C), 58.9 (ArCH_2), 51.4 (NCH_2CH$_3$), 46.3 [N(CH$_3$)$_2$], 42.8 [C(CH$_3$)$_2$Ph], 42.6 [C(CH$_3$)$_2$Ph], 31.7 [C(CH$_3$)$_2$Ph], 31.4 [C(CH$_3$)$_2$Ph], 27.2 (NCH$_2$CH$_3$), 20.4 (ArCH$_3$), 20.0 (ArCH$_3$), 6.5 (SiCH$_3$) ppm. $C_{49}H_{67}N_3OSi_2Zn$ (835.64): calcd. C 70.43, H 8.08, N 5.03; found C 70.05, H 8.01, N 4.70.

[(L^5)ZnN(SiMe$_3$)$_2$] (5b): A similar method was employed as that described for **1b**. **L^{5}H** (0.683 g, 1.00 mmol) was treated with Zn[N(SiMe$_3$)$_2$]$_2$ (0.386 g, 1.00 mmol) in toluene (15 mL) at room temp. to give a foamlike material. Recrystallization from toluene/hexane afforded colorless crystals as complex **5b** (503 mg, 55.5 %), m.p. 111–113 °C. ^{1}H NMR (C_6D_6, 400 MHz): δ = 7.61–7.52 (m, 7 H, ArH), 7.50 (d, J = 8.2 Hz, 1 H, ArH), 7.36 (t, J = 7.5 Hz, 2 H, ArH), 7.18–7.09 (m, 1 H, ArH), 7.06–6.99 (m, 1 H, ArH), 6.94 (t, J = 7.4 Hz, 1 H, ArH), 6.80 (d, J = 7.7 Hz, 2 H, ArH), 6.71 (t, J = 7.7 Hz, 1 H, ArH), 6.59 (t, J = 7.7 Hz, 1 H, ArH), 6.37 (t, J = 7.2 Hz, 1 H, ArH), 6.28 (d, J = 8.7 Hz, 2 H, ArH), 6.18 (t, J = 7.6 Hz, 2 H, ArH), 4.74 (d, J = 14.9 Hz, 1 H, ArCH_2), 4.08 (d, J = 15.0 Hz, 1 H, ArCH_2), 3.05–2.99 (m, 1 H, NCH_2CH$_3$), 2.75–2.66 (m, 1 H, NCH_2CH$_3$), 2.63 [s, 3 H, N(CH$_3$)$_2$], 2.14 [s, 3 H, C(CH_3)$_2$Ph], 1.88 [s, 3 H, C(CH_3)$_2$Ph], 1.86 [s, 3 H, C(CH_3)$_2$Ph], 1.54 [s, 3 H, N(CH$_3$)$_2$], 1.46 [s, 3 H, C(CH_3)$_2$Ph], 0.42 (t, J = 7.2 Hz, 3 H, NCH$_2$CH_3), 0.40 [s, 9 H, Si(CH$_3$)$_3$], –0.07 [s, 9 H, Si(CH$_3$)$_3$] ppm. ^{13}C NMR (C_6D_6, 100 MHz): δ = 162.8, 154.0, 153.5, 146.0, 141.4, 136.7, 135.7, 135.5, 134.4, 132.0, 131.7, 130.5, 129.5, 129.4, 129.3, 128.5, 128.2, 128.1, 127.6, 127.4, 127.2, 126.9, 126.8, 126.4, 126.2, 126.1, 125.9, 125.8, 125.7, 125.6, 124.0, 121.5, 118.8 (all Ar C), 59.3 (ArCH_2), 51.4 (NCH_2CH$_3$), 46.9 [N(CH$_3$)$_2$], 42.8 [C(CH$_3$)$_2$Ph], 42.7 [C(CH$_3$)$_2$Ph], 31.7 [C(CH$_3$)$_2$Ph], 31.5 [C(CH$_3$)$_2$Ph], 27.3 (NCH$_2$CH$_3$), 6.4 (SiCH$_3$) ppm (for clarity, solvent signals are not indicated in the NMR spectroscopic data). $C_{55}H_{67}N_3OSi_2Zn$·0.6hexane: calcd. C 73.36, H 7.92, N 4.38; found C 73.26, H 7.50, N 4.04.

X-ray Diffraction: Suitable single crystals of complexes **1b**, **3b**, **5a**, and **5b** for X-ray diffraction analysis were obtained from saturated solutions in toluene/hexane at room temperature. Diffraction data were collected with a Bruker Smart 1000 CCD diffractometer with graphite-monochromated Mo-K_α (λ = 0.71073 Å) radiation. All data were collected at 140 or 293 K by using the ω-scan technique. All structures were solved by direct methods and refined by Fourier techniques. An absorption correction based on SADABS was applied.[76] All non-hydrogen atoms were refined by full-matrix least-squares methods on F^2 by using the SHELXTL program package.[77] Hydrogen atoms were located and refined by geometric method. The cell refinement, data collection, and reduction were done with Bruker SAINT.[78] The structure solution and refinement were performed with SHELXL-97[79] and SHELXL-2013. SQUEEZE was used for **5a**, **3b**, and **5b**, OLEX2 was used for **1b**. Molecular structures were generated with ORTEP III.[80] For complex **1b**: $C_{47}H_{63}N_3OSi_2Zn$; triclinic, $P\bar{1}$; a = 13.2300(18), b = 13.3702(18), c = 15.751(2) Å; α = 80.986(3), β = 82.522(3), γ = 66.010(2)°; Z = 2. For complex **3b**: $C_{55}H_{81}N_3OSi_2Zn$; triclinic, $P\bar{1}$; a = 13.0326(16), b = 14.5796(18), c = 16.981(2) Å; α = 104.916(2), β = 103.356(3), γ = 104.166(2)°; Z = 2. For complex **5a**: $C_{55}H_{67}MgN_3OSi_2$; triclinic, $P\bar{1}$; a = 12.278(2), b = 15.122(3), c = 17.749(5) Å; α = 97.615(4), β = 100.073(4), γ = 111.948(3)°; Z = 2. For complex **5b**: $C_{55}H_{67}N_3OSi_2Zn$; triclinic, $P\bar{1}$; a = 12.252(8), b = 15.016(10), c = 17.599(12) Å; α = 98.158(13), β = 99.532(14), γ = 112.005(11)°; Z = 2.

CCDC 1041588 (for **1b**), 1041589 (for **3b**), 1041590 (for **5a**), and 1041591 (for **5b**) contain the supplementary crystallographic data for this paper. These data can be obtained free of charge from The Cambridge Crystallographic Data Centre.

Typical Polymerization Procedure: In a Braun Labstar glove box, initiator solution (0.5 mL, 0.01 M) in THF or toluene was injected sequentially into a series of 10 mL Schlenk tubes loaded with *rac*-LA (0.144 g, 1.00 mmol) or α-MeTMC (0.116 g, 1.00 mmol) and suitable amounts of dry solvent. Then, each Schlenk tube was taken out of the glove box and immersed in an oil bath thermostatted at 25 °C or 50 °C for polymerization. The reaction mixture was quenched at appropriate time intervals by adding wet petroleum ether and then extracted with CH_2Cl_2. Monomer conversion was monitored by ^{1}H NMR spectroscopy after removal of all the volatile substances of the withdrawn aliquot. The bulk solution was treated with an excess of methanol and the precipitated polymer was collected. The obtained polymers were dried in a vacuum oven at 60 °C for 24 h.

In the cases in which 2-propanol was used, the solution of the initiator was injected into the solution of the monomer in toluene to which 2-propanol was added. Otherwise the procedures were the same.

Acknowledgments

This work was subsidized by the National Natural Science Foundation of China (NNSFC) (grant numbers 21074032 and 21474028), and the Fundamental Research Funds for the Central Universities (grant number WD1113011). All the financial support is gratefully acknowledged.

Keywords: Polymerization · Ring-opening polymerization · Magnesium · Zinc · Tridentate ligands · N,O ligands

[1] R. E. Drumright, P. R. Gruber, D. E. Henton, *Adv. Mater.* **2000**, *12*, 1841–1846.
[2] G. W. Coates, M. A. Hillmyer, *Macromolecules* **2009**, *42*, 7987–7989.
[3] C. M. Thomas, *Chem. Soc. Rev.* **2010**, *39*, 165–173.
[4] M. J. Stanford, A. P. Dove, *Chem. Soc. Rev.* **2010**, *39*, 486–494.
[5] F. M. García-Valle, R. Estivill, C. Gallegos, T. Cuenca, M. E. G. Mosquera, V. Tabernero, J. Cano, *Organometallics* **2015**, *34*, 477–487.
[6] E. Kober, R. Petrus, P. Kociecka, Z. Janas, P. Sobota, *Polyhedron* **2015**, *85*, 814–823.
[7] J.-J. Zhang, J. Xiong, Y.-Y. Sun, N. Tang, J.-C. Wu, *Macromolecules* **2014**, *47*, 7789–7796.
[8] N. Spassky, M. Wisniewski, C. Pluta, A. LeBorgne, *Macromol. Chem. Phys.* **1996**, *197*, 2627–2637.
[9] T. M. Ovitt, G. W. Coates, *J. Am. Chem. Soc.* **2002**, *124*, 1316–1326.
[10] Z. Zhong, P. J. Dijkstra, J. Feijen, *J. Am. Chem. Soc.* **2003**, *125*, 11291–11298.
[11] P. Hormnirun, E. L. Marshall, V. C. Gibson, A. J. P. White, D. J. Williams, *J. Am. Chem. Soc.* **2004**, *126*, 2688–2689.
[12] H.-L. Chen, S. Dutta, P.-Y. Huang, C.-C. Lin, *Organometallics* **2012**, *31*, 2016–2025.
[13] B. Gao, X. Li, R. L. Duan, Q. Duan, Y. H. Li, X. Pang, H. J. Zhuang, X.-S. Chen, *RSC Adv.* **2015**, *5*, 29412–29419.
[14] A. Pilone, K. Press, I. Goldberg, M. Kol, M. Mazzeo, M. Lamberti, *J. Am. Chem. Soc.* **2014**, *136*, 2940–2943.
[15] A. Pilone, N. D. Maio, K. Press, V. Venditto, D. Pappalardo, M. Mazzeo, C. Pellecchia, M. Kol, M. Lamberti, *Dalton Trans.* **2015**, *44*, 2157–2165.
[16] A. B. Biernesser, B. Li, J. A. Byers, *J. Am. Chem. Soc.* **2013**, *135*, 16553–16560.
[17] C. M. Manna, H. Z. Kaplan, B. Li, J. A. Byers, *Polyhedron* **2014**, *84*, 160–167.
[18] A. Sauer, A. Kapelski, C. Fliedel, S. Dagorne, M. Kol, J. Okuda, *Dalton Trans.* **2013**, *42*, 9007–9023.
[19] B. Gao, X. Li, R. L. Duan, X. Pang, *New J. Chem.* **2015**, *39*, 2404–2408.
[20] B. Gao, Q. Duan, Y. H. Li, D. N. Li, L. Q. Zhang, Y. Cui, N. H. Hu, X. Pang, *RSC Adv.* **2015**, *5*, 13437–13442.
[21] M. D. Jones, S. L. Hancock, P. McKeown, P. M. Schäfer, A. Buchard, L. H. Thomas, M. F. Mahon, J. P. Lowe, *Chem. Commun.* **2014**, *50*, 15967–15970.
[22] A. Stopper, J. Okuda, M. Kol, *Macromolecules* **2012**, *45*, 698–704.
[23] W.-C. Hung, C.-C. Lin, *Inorg. Chem.* **2009**, *48*, 728–734.
[24] L. Wang, H. Ma, *Macromolecules* **2010**, *43*, 6535–6537.
[25] S. Song, H. Ma, Y. Yang, *Dalton Trans.* **2013**, *42*, 14200–14211.
[26] Y. Gao, Z.-G. Dai, J.-J. Zhang, X.-X. Ma, N. Tang, J.-C. Wu, *Inorg. Chem.* **2014**, *53*, 716–726.
[27] B. Gao, D.-H. Zhao, X. Li, Y. Cui, R.-L. Duan, X. Pang, *RSC Adv.* **2015**, *5*, 440–447.
[28] M. H. Chisholm, K. Choojun, J. C. Gallucci, P. M. Wambua, *Chem. Sci.* **2012**, *3*, 3445–3457.
[29] R. A. Collins, J. Unruangsri, P. Mountford, *Dalton Trans.* **2013**, *42*, 759–769.
[30] Y. Huang, W. Wang, C.-C. Lin, M. P. Blake, L. Clark, A. D. Schwarz, P. Mountford, *Dalton Trans.* **2013**, *42*, 9313–9324.
[31] Y. Sarazin, B. Liu, T. Roisnel, L. Maron, J.-F. Carpentier, *J. Am. Chem. Soc.* **2011**, *133*, 9069–9087.
[32] C. Y. Li, P. S. Chen, S. J. Hsu, C. H. Huang, B. T. KO, *J. Organomet. Chem.* **2012**, *716*, 175–181.
[33] C.-Y. Sung, C.-Y. Li, J.-K. Su, T.-Y. Chen, C.-H. Lin, B.-T. Ko, *Dalton Trans.* **2012**, *41*, 953–961.
[34] T. J. J. Whitehorne, B. Vabre, F. Schaper, *Dalton Trans.* **2014**, *43*, 6339–6352.
[35] W.-L. Kong, Z.-X. Wang, *Dalton Trans.* **2014**, *43*, 9126–9135.
[36] D. J. Darensbourg, O. Karroonnirun, *Inorg. Chem.* **2010**, *49*, 2360–2371.
[37] N. M. Rezayee, K. A. Gerling, A. L. Rheingold, J. M. Fritsch, *Dalton Trans.* **2013**, *42*, 5573–5586.
[38] B. Gao, R.-L. Duan, X. Pang, X. Li, Z. Qu, H.-L. Shao, X.-H. Wang, X.-S. Chen, *Dalton Trans.* **2013**, *42*, 16334–16342.
[39] K. A. Gerling, N. M. Rezayee, A. L. Rheingold, D. B. Greena, J. M. Fritsch, *Dalton Trans.* **2014**, *43*, 16498–16508.
[40] K. S. Kwon, S. Nayab, H. Lee, J. H. Jeong, *Polyhedron* **2014**, *77*, 32–38.
[41] M. Honrado, A. Otero, J. Fernández-Baeza, L. F. Sánchez-Barba, A. Garcés, A. Lara-Sáncheza, A. M. Rodrígueza, *Dalton Trans.* **2014**, *43*, 17090–17100.
[42] M. J. Walton, S. J. Lancaster, J. A. Wright, M. R. J. Elsegood, C. Redshaw, *Dalton Trans.* **2014**, *43*, 18001–18009.
[43] D. J. Darensbourg, W. Choi, O. Karroonnirun, N. Bhuvanesh, *Macromolecules* **2008**, *41*, 3493–3502.
[44] M. G. Cushion, P. Mountford, *Chem. Commun.* **2011**, *47*, 2276–2278.
[45] P. Horeglad, G. Szczepaniak, M. Dranka, J. Zachara, *Chem. Commun.* **2012**, *48*, 1171–1173.
[46] M.-W. Hsiao, C.-C. Lin, *Dalton Trans.* **2013**, *42*, 2041–2051.
[47] S. Sun, K. Nie, Y. F. Tan, B. Zhao, Y. Zhang, Q. Shen, Y.-M. Yao, *Dalton Trans.* **2013**, *42*, 2870–2878.
[48] C. Bakewell, T.-P.-A. Cao, N. Long, X. F. Le Goff, A. Auffrant, C. K. Williams, *J. Am. Chem. Soc.* **2012**, *134*, 20577–20580.
[49] M. V. Yakovenko, A. A. Trifonov, J.-F. Carpentier, *Inorg. Chim. Acta* **2012**, *383*, 137–142.
[50] M. Zhang, X. F. Ni, Z. Q. Shen, *Organometallics* **2014**, *33*, 6861–6867.
[51] H. Xie, Z. Mou, B. Liu, P. Li, W. Rong, S. Li, D. Cui, *Organometallics* **2014**, *33*, 722–730.
[52] F. Drouin, P. O. Oguadinma, T. J. J. Whitehorne, R. E. Prud"homme, F. Schaper, *Organometallics* **2010**, *29*, 2139–2147.
[53] S. Abbina, G. Du, *ACS Macro Lett.* **2014**, *3*, 689–692.
[54] D. J. Darensbourg, O. Karroonnirun, S. J. Wilson, *Inorg. Chem.* **2011**, *50*, 6775–6787.
[55] P. Brignou, S. M. Guillaume, T. Roisnel, D. Bourissou, J.-F. Carpentier, *Chem. Eur. J.* **2012**, *18*, 9360–9370.
[56] K. Makiguchi, Y. Ogasawara, S. Kikuchi, T. Satoh, T. Kakuchi, *Macromolecules* **2013**, *46*, 1772–1782.
[57] B. Liu, T. Roisnel, L. Maron, J.-F. Carpentier, Y. Sarazin, *Chem. Eur. J.* **2013**, *19*, 3986–3994.
[58] H. Yasuda, M.-S. Aludin, N. Kitamura, M. Tanabe, H. Sirahama, *Macromolecules* **1999**, *32*, 6047–6057.
[59] J. Ling, Y. Dai, Y. Zhu, W. Sun, Z. Shen, *J. Polym. Sci., Part A J. Polym. Sci. A Polym. Chem.* **2010**, *48*, 3807–3815.
[60] P. Brignou, J.-F. Carpentier, S. M. Guillaume, *Macromolecules* **2011**, *44*, 5127–5135.
[61] W. Yi, H. Ma, *Dalton Trans.* **2014**, *43*, 5200–5210.
[62] M. Huang, C. Pan, H. Ma, *Dalton Trans.* **2015**, *44*, 12420–12431.
[63] These aminophenol proligands are very unstable to column chromatography (both on Al_2O_3 and silica), and complete decomposition occurred if the whole procedure took longer than 10 min. Therefore, satisfactory elemental analysis was only obtained occasionally.
[64] Aminophenols of the same type but with sterically less bulky *ortho*-substituents (e.g., *o*-Cl, *o*-Br, *o*-*t*Bu) were also obtained and treated with $Mg[N(SiMe_3)_2]_2$ or $Zn[N(SiMe_3)_2]_2$. However, all reactions failed to afford the target heteroleptic complexes.
[65] Z. Y. Zhong, P. J. Dijkstra, J. Feijen, *Angew. Chem. Int. Ed.* **2002**, *114*, 4510–4513; *Angew. Chem.* **2002**, *114*, 4692.
[66] H. Z. Du, A. H. Velders, P. J. Dijkstra, J. R. Sun, Z. Y. Zhong, X. S. Chen, J. Feijen, *Chem. Eur. J.* **2009**, *15*, 9836–9845.
[67] C. K. Williams, L. E. Breyfogle, S. K. Choi, W. Nam, V. G. Young Jr., M. A. Hillmyer, W. B. Tolman, *J. Am. Chem. Soc.* **2003**, *125*, 11350–11359.
[68] H.-Y. Chen, H.-Y. Tang, C.-C. Lin, *Macromolecules* **2006**, *39*, 3745–3752.
[69] A. Sauer, A. J.-C. Buffet, T. P. Spaniol, H. Nagae, K. Mashima, J. Okuda, *Inorg. Chem.* **2012**, *51*, 5764–5770.
[70] W. Yi, H. Ma, *Inorg. Chem.* **2013**, *52*, 11821–11835.
[71] L. E. Breyfogle, C. K. Williams, V. G. Young Jr., M. A. Hillmyer, W. B. Tolman, *Dalton Trans.* **2006**, *35*, 928–936.
[72] Y. Huang, W. Wang, C.-C. Lin, M. P. Blake, L. Clark, A. D. Schwarz, P. Mountford, *Dalton Trans.* **2013**, *42*, 9313–9324.
[73] K. Karlheinz, W. Niell, *Chem. Ber.* **1963**, *96*, 1877–1880.
[74] H. Bürger, W. Sawodny, U. Wannagat, *J. Organomet. Chem.* **1965**, *3*, 113–120.
[75] Y. Wang, H. Ma, *Chem. Commun.* **2012**, *48*, 6729–6731.
[76] *SADABS*, *Bruker Nonius area detector scaling and absorption correction*, version 2.05, Bruker AXS Inc., Madison, WI, USA, **1996**.

[77] G. M. Sheldrick, *SHELXTL*, version 5.10 for Windows NT, *Structure Determination Software Programs*, Bruker Analytical X-ray Systems, Inc., Madison, WI, USA, **1997**.
[78] *SAINT*, version 6.02, Bruker AXS Inc., Madison WI, USA, **1999**, 53711–5373.
[79] G. M. Sheldrick, *SHELXS-97*, *Program for the Solution of Crystal Structures*, University of Göttingen, Germany, **1990**.
[80] L. J. Farrugia, *J. Appl. Crystallogr.* **1997**, *30*, 565; *ORTEP-III for Windows*, version 2.0, University of Glasgow, UK, **2008**.

Received: April 15, 2016
Published Online: July 14, 2016